UAV for Terrain Mapping

A THESIS SUBMITTED IN PARTIAL FULFILLMENT OF THE REQUIREMENTS FOR THE DEGREE OF

Bachelors of Engineering (Mechatronics)

By

M. Osama Horani 1945154
Mariya Najeeb 1945107
Affan Ahmed 1945123

Under supervision of

Dr. M. Umar Siddiqui

Shaheed Zulfiqar Ali Bhutto Institute of Science & Technology
Faculty of Mechatronics Engineering Karachi, Pakistan

August 2023

Abstract

This thesis report aims to address the need for accurate and efficient terrain mapping by designing, implementing, and flight testing an unmanned aerial vehicle system. The study focuses on the background and context of the research, highlighting the importance of addressing this topic. By filling a gap in previous research and applying new methods, the study seeks to provide valuable insights and solutions. The research methodology involves designing a fixed-wing UAV with essential hardware components and conducting flight tests to evaluate its performance and stability. The main findings reveal the successful integration of a high-resolution camera, flight controller, and sensors for data capture. The UAV's autonomous navigation and precise positioning capabilities enable comprehensive terrain coverage. The data collected is processed using Pix4D to generate accurate 3D terrain models. The significance of these findings lies in their potential applications, including urban planning, environmental monitoring, and disaster management. This research contributes to the field by offering a practical and effective approach to terrain mapping, demonstrating the feasibility and value of UAV-based photogrammetry.

Acknowledgements

We gratefully acknowledge Dr. M. Umar Siddiqui, our esteemed supervisor, for his invaluable guidance and unwavering support throughout this project. His expertise and advice have played a pivotal role in shaping our work. Our deepest appreciation goes to the committee members for their recognition and approval of our project thesis. We would also like to extend our sincere thanks to Ms. Tanzila for her invaluable assistance in ensuring the timely progress and smooth execution of our project. Lastly, we are profoundly grateful to our families, whose unwavering support has been a cornerstone throughout our academic journey. Their understanding, encouragement, and sacrifices have enabled us to devote countless hours to our studies at the university.

Table of Contents

List of Figures

Nomenclature

Acronyms

UAV	Unmanned Aerial Vehicle
FBWA	Fly by Wire A
LIDAR	Light Detection and Ranging
MH60	Martin Hepperle 60
Cl	Coefficient of Lift
Cd	Coefficient of Drag
Cp	Pressure Coefficient
AoA	Angle of Attack
EPP	Expanded Polypropylene
XPS	Extruded Polystyrene
BLDC	Brushless DC
LIPO	Lithium Polymer
GPS	Global Positioning System
ESC	Electronic Speed Controller
UBEC	Universal Battery Eliminator Circuit

Units

kV	RPM per Volt
C	Rate at which battery will charge or discharge
mAh	Milli Amperes per Hour

Chapter 1

Introduction

1.1 Overview

Fixed-wing unmanned aerial vehicles (UAVs) have revolutionized the field of terrain mapping and photogrammetry. Together, these technologies enable the capture of high-resolution imagery and elevation data, enabling the creation of accurate 3D maps and models of various terrains. The adoption of fixed-wing UAVs using photogrammetry has grown significantly in recent years [12].

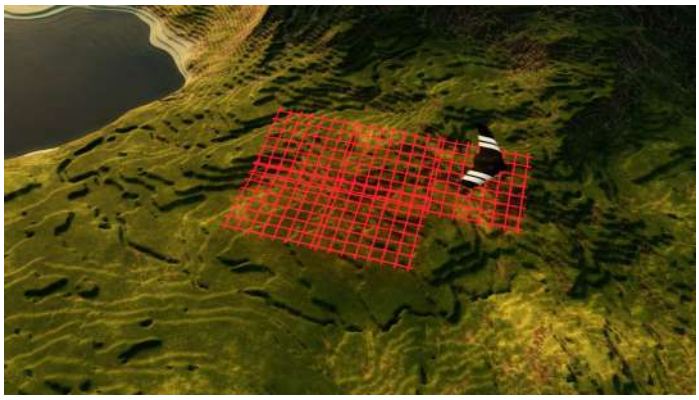

FIGURE 1.1: Terrain Mapping Render

1.2 Background

Fixed-wing UAVs have also come a long way in recent years, with technological advances enabling increased payload capacity, longer flight times, and more accurate navigation systems. The integration of photogrammetry and fixed-wing UAVs has brought new levels of accuracy and efficiency to terrain mapping. UAVs eliminate the need for manned aircraft, reduce costs, improve accessibility, and provide real-time data processing and visualization capabilities. Photogrammetry is a branch of geography that deals with extracting information from images. Photogrammetric terrain mapping involves taking aerial photographs of a specific area and processing them with special software to create accurate 3D models and maps of the terrain. Over the years, photogrammetry has evolved with advances in technology to provide more efficient and cost-effective solutions for terrain mapping [17]. Figure 1.1 displays a render of the UAV taking images of the land to be processed for the creation of terrain models. In summary, the combination of fixed-wing UAVs and photogrammetry

paves the way for a new era of terrain mapping, providing efficient and cost-effective solutions for a wide variety of applications. This review article discusses the latest advances in this field and provides an overview of the state-of-the-art in fixed-wing UAVs for terrain mapping using photogrammetry.

1.3 Current State of The Art

In recent years, significant progress has been made in using fixed-wing UAVs for terrain mapping using photogrammetry. Advances in photogrammetry software, UAV hardware, and navigation systems have increased the accuracy, efficiency, and affordability of terrain mapping [25]. The availability of high-definition cameras and multispectral sensors has enabled the collection of more detailed data, enabling the creation of highly accurate 3D maps and models of various terrains [8]. In addition, the integration of machine learning algorithms has increased the speed and accuracy of data processing and analysis, enabling real-time data visualization and analysis [5].

1.4 Motivation

The increasing adoption of fixed-wing UAVs for terrain mapping using photogrammetry emphasizes the need for a comprehensive review of the latest advances in this field. This review paper aims to provide a comprehensive overview of the state-of-the-art in fixed-wing UAVs for terrain mapping using photogrammetry, highlighting recent advances, limitations, and future directions. increase. This will provide valuable insights to researchers, practitioners, and stakeholders in the field to facilitate the development and deployment of these technologies.

1.5 Statement of the Problem

The statement of the problem for this project is **the need for accurate and efficient terrain mapping for various applications such as land surveying, environmental**

FIGURE 1.2: Requirement of identification of flood-prone areas

monitoring, and disaster management. Traditional ground-based surveying methods are time-consuming and expensive, and may not be practical for large or remote areas [14].

Figure 1.2 shows a satellite image of a village before and after a thunderstorm. It conveys the need for methods to identify flood prone areas to prevent the destruction of infrastructure and loss of lives. Aerial photogrammetry using unmanned aerial vehicles (UAVs) has emerged as a promising solution to this problem. However, most UAVs used for terrain mapping are multi-rotor drones, which have limited range and endurance. This project aims to address this problem by designing and building a fixed-wing UAV optimized for terrain mapping using photogrammetry. The goal is to achieve longer flight times and wider coverage areas while maintaining high accuracy and resolution in the resulting terrain models.

1.6 Solution to the problem

This project aims to address this problem by designing and building a fixed-wing UAV optimized for terrain mapping using photogrammetry. The goal is to achieve longer flight times and wider coverage areas while maintaining high accuracy and resolution in the resulting terrain models.

1.7 Objectives

The objectives of the project are to design, build, and test a fixed-wing UAV for terrain mapping using photogrammetry. Specifically, the project aims to:

1. Design and build a fixed-wing UAV from scratch with a focus on aerodynamic performance, stability, and endurance.

2. Develop a photogrammetry-based mapping system to capture high-resolution aerial images of a designated area.

3. Integrate the mapping system with the UAV to facilitate autonomous flight and data collection.

4. Conduct flight tests to evaluate the performance and accuracy of the mapping system and the UAV as a whole.

5. Generate a 3D terrain model of the designated area using the collected data and evaluate the accuracy and quality of the model.

6. Analyze the results and identify opportunities for further improvement in the UAV design and mapping system.

1.8 Application

The applications of the fixed-wing UAV used for terrain mapping using photogrammetry are vast and varied. The project can be applied in the fields of agriculture, forestry, environmental monitoring, mining, urban planning, disaster management, and more.

One of the primary applications of the fixed-wing UAV is in agriculture. It can be used for monitoring crop growth, identifying plant diseases, and assessing soil quality, which can help farmers increase their crop yields and reduce costs [11]. The UAV can also be used for forestry management, by providing accurate 3D maps of forested areas, allowing forest managers to monitor the growth and health of the forest, track wildlife habitats, and assess timber resources. In environmental monitoring, the UAV can be used to track changes in land use, monitor biodiversity, and even monitor the impact of climate change.

In the mining industry, fixed-wing UAVs can be used to create detailed maps of mining sites, monitor the progress of mining activities, and ensure the safety of workers. Additionally, the technology can be used in urban planning to create accurate and up-to-date

maps of cities, identify areas that require improvement, and facilitate the planning and development of infrastructure. The project can also be used in disaster management, where it can provide valuable information about disaster-affected areas and help identify areas where rescue and relief efforts are needed.

1.9 Sustainable Development Goals

There are several UN Sustainable Development Goals (SDGs) that can be assigned to this project.

- First, SDG 9: Industry, Innovation, and Infrastructure, as the project involves designing and developing a fixed-wing UAV for terrain mapping using photogrammetry. The project contributes to developing and enhancing innovative infrastructure to support sustainable development.

- Second, SDG 11: Sustainable Cities and Communities, as the technology can be used for urban planning, disaster management, and monitoring environmental changes. This supports the goal of creating sustainable and resilient cities and communities.

- Third, SDG 13: Climate Action, as the technology can help monitor and assess environmental changes and support efforts to reduce greenhouse gas emissions. The project can contribute to the goal of taking urgent action to combat climate change and its impacts.

- Fourth, SDG 15: Life on Land, as the technology can be used for environmental monitoring and conservation efforts, such as tracking changes in forest cover and identifying wildlife habitats. The project can contribute to protecting, restoring, and promoting the sustainable use of terrestrial ecosystems and biodiversity.

Overall, this project has the potential to contribute to several sustainable development goals by providing a cost-effective and efficient technology for terrain mapping and environmental monitoring.

1.10 Environmental, Social, Health, and Safety Impacts

The use of fixed-wing UAVs for terrain mapping using photogrammetry has several environmental, social, health, and safety impacts.

In terms of environmental impacts, the use of UAVs reduces the need for ground-based survey methods, which can cause damage to ecosystems and habitats. Fixed-wing UAVs have a lower carbon footprint compared to manned aircraft, which can contribute to air pollution and climate change. The use of photogrammetry also reduces the need for physical markers, which can be harmful to the environment. However, the use of lithium-ion batteries in UAVs can cause environmental damage when not properly disposed of or recycled [8].

In terms of social impacts, the use of UAVs for terrain mapping can provide accurate and up-to-date information on land and infrastructure, which can be used to aid in disaster response and planning. However, there may be concerns about privacy and surveillance when using UAVs for mapping.

In terms of health and safety impacts, the use of UAVs for terrain mapping can reduce the need for human workers to physically survey areas, which can be dangerous or difficult to access. However, there are safety concerns related to the operation of UAVs, such as the risk of collisions and the potential for injuries if the UAV malfunctions or crashes. There are also concerns about the potential for cyber attacks on the UAV's control systems. Proper safety measures and training must be put in place to mitigate these risks.

Chapter 2

Literature Review

2.1 Literature Review

Unmanned Aerial Vehicles (UAVs) have become increasingly popular in the field of remote sensing for their ability to collect high-resolution data in a cost-effective and efficient manner. Among the different types of UAVs, fixed-wing UAVs have been particularly useful for terrain mapping due to their longer flight times and larger coverage area compared to rotary-wing UAVs. In addition, photogrammetry, a remote sensing technique that uses images to create 3D models of terrain features, has been widely used for mapping terrain with fixed-wing UAVs. This literature review aims to discuss the advantages of using fixed-wing UAVs and photogrammetry for terrain mapping, their applications, and their importance in different fields.

Fixed wing UAVs have several advantages over rotary-wing UAVs for terrain mapping. First, fixed-wing UAVs have longer flight times due to their aerodynamic design and efficient engines, enabling them to cover larger areas in a single flight [1]. Second, fixed-wing UAVs can fly at higher altitudes, allowing them to capture a larger area in a single image and reducing the number of images needed to cover a given area [2]. Third, fixed-wing UAVs are less affected by wind, which can cause instability in rotary-wing UAVs [3]. Fourth, fixed-wing UAVs are more stable and can fly in straight lines, which is important for photogrammetry since it requires images to be taken at specific angles and distances [4].

Photogrammetry has several advantages over other remote sensing techniques for terrain mapping. First, photogrammetry can provide high-resolution 3D models of terrain features with high accuracy [5]. Second, photogrammetry is a cost-effective method for terrain mapping since it does not require expensive equipment or extensive fieldwork [6]. Third, photogrammetry can be used to create orthophotos, which are corrected for distortions and provide accurate measurements of distances, angles, and areas [7]. Fourth, photogrammetry can be used to monitor changes in terrain features over time by comparing 3D models generated from images taken at different times [8].

Fixed-wing UAVs and photogrammetry have a wide range of applications for terrain mapping. In agriculture, fixed-wing UAVs can be used to monitor crop growth and detect crop diseases, pests, and nutrient deficiencies [9]. In environmental monitoring, fixed-wing UAVs can be used to monitor and manage forest fires, floods, and landslides [10]. In

urban planning, fixed-wing UAVs and photogrammetry can be used to create 3D models of buildings and infrastructure for city planning and development [11]. In archaeology, fixed-wing UAVs and photogrammetry can be used to create detailed maps of archaeological sites and monuments [12]. In geology, fixed-wing UAVs and photogrammetry can be used to map geological formations and monitor landslides and erosion [13].

Fixed-wing UAVs and photogrammetry are important for terrain mapping in several ways. First, they provide a cost-effective and efficient method for collecting high-resolution data, enabling researchers to cover larger areas in less time and at a lower cost [14]. Second, they can provide detailed and accurate maps of terrain features, which can be used for monitoring and management of natural resources, disaster response, and urban planning [15]. Third, they can provide important information for decision-making processes in different fields, including agriculture, environmental monitoring, urban planning, archaeology, and geology [16]. Fixed-wing UAVs have become increasingly popular in recent years, especially in the field of terrain mapping. One of the main advantages of using a fixed-wing UAV for mapping is its ability to cover large areas efficiently and quickly [14]. Fixed-wing UAVs are more efficient than other UAVs such as rotary wings or quadcopters in terms of endurance, range, and stability [15]. Furthermore, fixed-wing UAVs are capable of flying at higher altitudes, resulting in higher-resolution images [16].

When it comes to photogrammetry, it is a method for generating a 3D model of terrain through photographs taken from different angles [17]. Photogrammetry has been used in various fields, including cartography, geology, and civil engineering [18]. By using photogrammetry, it is possible to obtain high-resolution 3D models of the terrain with high accuracy [19]. The accuracy of the model can be further improved by using Ground Control Points (GCPs) [20]. The GCPs are points on the terrain that have been precisely measured with a GPS and act as a reference for the photogrammetry software.

The combination of a fixed-wing UAV and photogrammetry is a powerful tool for terrain mapping, and many studies have been conducted in this area. In a study by Sulistyo et al., a fixed-wing UAV was used to create a 3D model of an archaeological site in Indonesia using photogrammetry [21]. The results showed that the use of a fixed-wing UAV allowed for the mapping of a large area in a short time. In another study by Cao et al., a fixed-wing UAV was used to create a 3D model of a quarry using photogrammetry [22]. The study

showed that the UAV was capable of mapping the terrain with high accuracy.

In addition to mapping, fixed-wing UAVs are also used in various applications such as surveillance, search and rescue, and environmental monitoring [23]. In a study by Zhang et al., a fixed-wing UAV was used for monitoring the water quality of a lake using a hyperspectral camera [24]. The results showed that the UAV was capable of detecting water quality parameters such as chlorophyll-a concentration with high accuracy.

The design of a fixed-wing UAV is an essential aspect of its performance in mapping and other applications. In a study by Soloviev et al., the authors designed a fixed-wing UAV for mapping and conducted aerodynamic analysis and simulation [25]. The results showed that the designed UAV had good aerodynamic performance and was capable of flying at high altitudes for a long time.

The flight controller is another crucial component of a fixed-wing UAV. In a study by Nayak et al., a Pixhawk flight controller was used in a fixed-wing UAV for terrain mapping using photogrammetry [26]. The study showed that the use of the Pixhawk flight controller allowed for stable and precise flight control of the UAV.

The integration of Unmanned Aerial Vehicles (UAVs) in terrain mapping and environmental monitoring has shown significant promise in providing high-resolution data for accurate mapping and analysis. While existing literature has highlighted the benefits of UAVs in producing digital elevation models and orthomosaics for a variety of applications, there are significant gaps in the research. To begin, comprehensive studies that investigate the full potential of UAVs in real-time data acquisition and analysis for diverse environmental monitoring purposes other than flood risk assessment are required. Second, research on optimizing UAV flight paths, sensor configurations, and data processing techniques remains limited, limiting their full utilization. Furthermore, there is a lack of standardization of methodologies and protocols for UAV-based terrain mapping, making it difficult to compare and verify results across studies. Addressing these gaps will not only advance UAV technology, but will also open up new avenues for efficient and cost-effective terrain mapping in a variety of industries, including agriculture, urban planning, and natural resource management.

In conclusion, the combination of a fixed-wing UAV and photogrammetry is a powerful

tool for terrain mapping and has been extensively studied in various applications. The design of the fixed-wing UAV, aerodynamic analysis, and the use of a precise flight controller are essential aspects of its performance. Future research should focus on developing more advanced fixed-wing UAVs and improving photogrammetry software to achieve higher accuracy and resolution in terrain mapping.

Chapter 3

Experimental

3.1 Design of Experiment

A design of experiments (DOE) approach can be used in the development and testing of a fixed-wing UAV designed for terrain mapping. In this approach, a set of variables and parameters can be identified and manipulated to optimize the performance and accuracy of the UAV in capturing data for photogrammetry-based terrain mapping.

The DOE approach involves planning and executing experiments that systematically change and measure the variables of interest while holding other factors constant. For example, the following variables can be considered in the design of experiments for a fixed-wing UAV used for terrain mapping:

- The altitude and speed of the UAV

- The camera settings and lens choice

- The type of terrain being mapped

- The weather conditions during the flight

- The size and weight of the UAV

- The type of flight controller used

By varying and controlling these parameters, the experiment can determine which combination of factors will produce the best results in terms of data quality, accuracy, and efficiency.

The design of experiments can also help identify and mitigate potential safety and reliability issues associated with UAV flight. By testing and optimizing the UAV under a range of conditions, engineers can ensure that the UAV is safe, reliable, and effective in capturing accurate and high-quality data for photogrammetry-based terrain mapping.

What this project entails is a set of parameters that have been deemed appropriate for an undergraduate-level project. The altitude and speed of the UAV would be set to a level where an advantage can be seen when compared to a multirotor UAV. The camera selected for the project is a Mapier Survey 3 as it allows a 14 Megapixel image and is sturdy and lightweight enough. At an altitude of 60m the image taken would cover an area of 45m x

35m. It also provides adequate images to produce an accurate model. The types of terrain mapped for the project would be, landscapes with not too tall obstructions in the way. The wingspan of the flying wing is 1 meter long and the weight is required to be below 3kg. The type of flight controller used is a Pixhawk which provides adequate sensor inputs and provides a stable flight experience.

3.1.1 Block Diagram

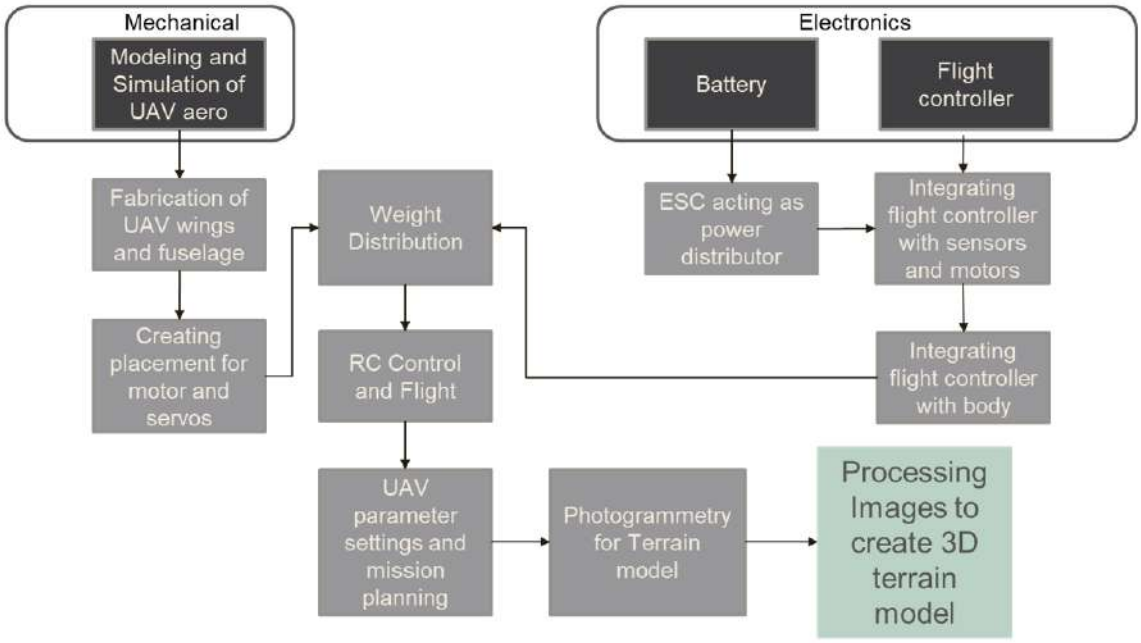

FIGURE 3.1: A Block Diagram for the project

In figure 3.1, The block diagram of the experiment shows the flow of information and control between these different components. The fixed-wing UAV captures images of the terrain using the camera and other sensors, which are transmitted to the ground control station for processing. The ground control station communicates with the flight controller to ensure the UAV is flying according to the pre-planned flight path. The images are then processed using photogrammetry software to create a 3D model of the terrain. The resulting 3D model can be used for a wide range of applications, such as urban planning, agriculture, and environmental monitoring.

3.2 Experimental Setup

3.2.1 Design and Modeling

Aircraft Design

The process of selecting an appropriate aircraft design began by considering the specific requirements that would yield optimal performance. After careful evaluation, it was determined that a flying wing design aligns most effectively with the project's objectives. The chosen design had to meet several criteria, including lightweight construction, the ability to operate without the need for a traditional runway, high-speed capabilities, low power consumption, and the capacity for hand launching. A flying wing design was deemed suitable since it eliminates the need for a tail section, including a rudder for yaw control. Control surfaces known as elevons, which combine elevator and aileron functionalities, are used. Moreover, the inherent aerodynamic characteristics of the flying wing design, particularly its improved performance under high wind speeds, make it highly suitable for flight requirements in the Karachi region. Figure 3.2 shows a preliminary design render of the flying wing aircraft.

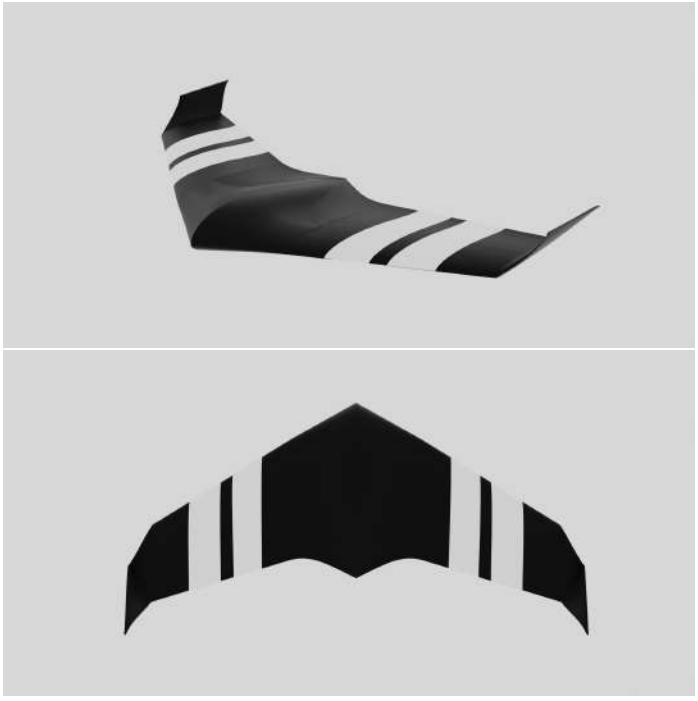

FIGURE 3.2: Side and top render of the flying wing model

One more design choice that had to be made for the aircraft design was its wing span. The span of an aircraft's wings determines its use case, the amount of surface area is directly proportional to the load it can handle, but it comes at a cost of increased power consumption as the weight increases. A wing span of 1 meter was selected as a decent length for a hand-launched flying wing.

Airfoil Selection

The airfoil selection of a flying wing is one of the most crucial aspects that determine the flight characteristics of the craft. An airfoil shape is used for the cross-section of the wing as it is the most efficient shape that can be used for an aircraft.

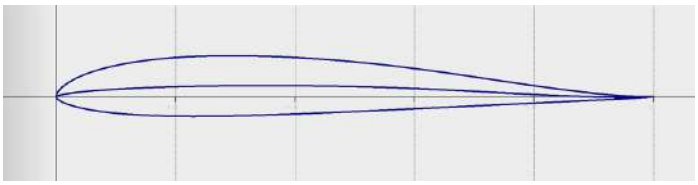

FIGURE 3.3: Shape of an MH60 Airfoil

A particular kind of airfoil is used for a flying wing called a reflexed airfoil. Figure 3.3 shows the MH60 reflex airfoil as a reference. These airfoils have a specific quality that fulfills the lack of a tail and stabilizes the aircraft using just its wings. These airfoils have a distinctive "s" shape which provides a moment in the positive direction to stabilize the wing.

When selecting an airfoil for a flying wing design, several critical parameters and associated graphs need to be studied to ensure optimal performance. The following factors and graphs are essential considerations for airfoil selection:

1. Lift Coefficient (Cl) vs. Angle of Attack (AoA) Graph (Figure 3.4): This graph represents the lift generated by the airfoil at different angles of attack. It is crucial to analyze the airfoil's performance across a range of AoA values to determine its lift characteristics and identify the maximum lift coefficient achievable before a stall occurs. 2. Drag Coefficient (Cd) vs. Angle of Attack (AoA) Graph (Figure 3.5): This graph illustrates the drag produced by the airfoil at different angles of attack. It is necessary to examine the air-

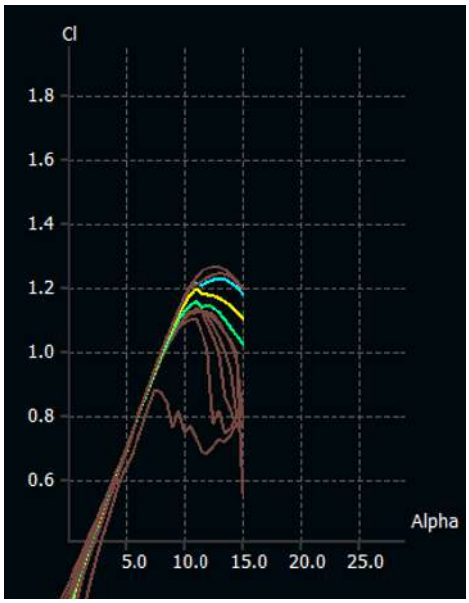

FIGURE 3.4: Cl vs. AoA for MH60

foil's drag behavior to identify the AoA range that provides the lowest drag coefficient and optimal aerodynamic efficiency. 3. Lift-to-Drag Ratio (L/D) vs. Angle of Attack (AoA)

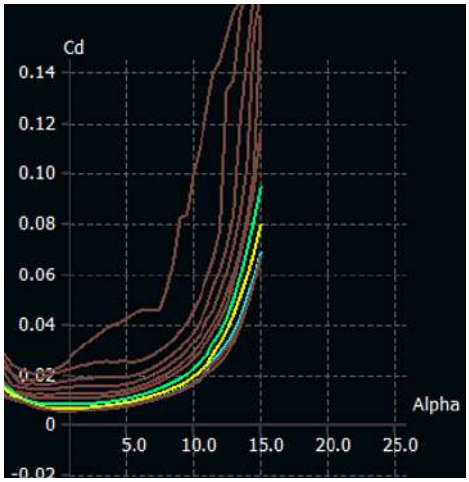

FIGURE 3.5: Cd vs. AoA for MH60

Graph (Figure 3.6): This graph depicts the ratio of lift to drag generated by the airfoil at various angles of attack. The L/D ratio serves as a measure of the airfoil's efficiency, with higher values indicating better performance. The graph assists in determining the AoA range where the airfoil achieves the highest L/D ratio. 4. Stall Angle: The stall angle is the angle of attack beyond which the smooth airflow over the airfoil's surface becomes turbulent, causing a significant reduction in lift and an increase in drag. It is essential to

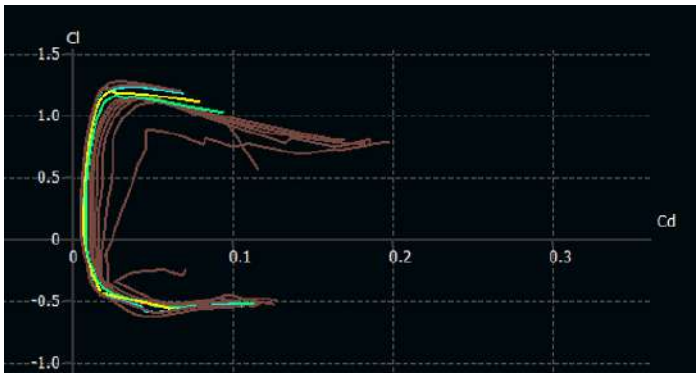

FIGURE 3.6: Cl vs. Cd for MH60

assess the airfoil's stall characteristics and select one that exhibits a relatively high stall angle, allowing for a wider range of operating angles of attack.

5. Camber and Thickness: The airfoil's camber refers to the curvature of the upper and lower surfaces, while thickness indicates the maximum distance between these surfaces. These parameters impact the lift and drag characteristics of the airfoil. The choice of camber and thickness should be based on the desired lift distribution, stability, and specific mission requirements.

6. Pressure Distribution (Figure 3.7): Analyzing the airfoil's pressure distribution helps understand how the flow behaves over its surface. Ideally, the airfoil should exhibit a favorable pressure distribution that promotes smooth and attached airflow, delaying stall and reducing drag.

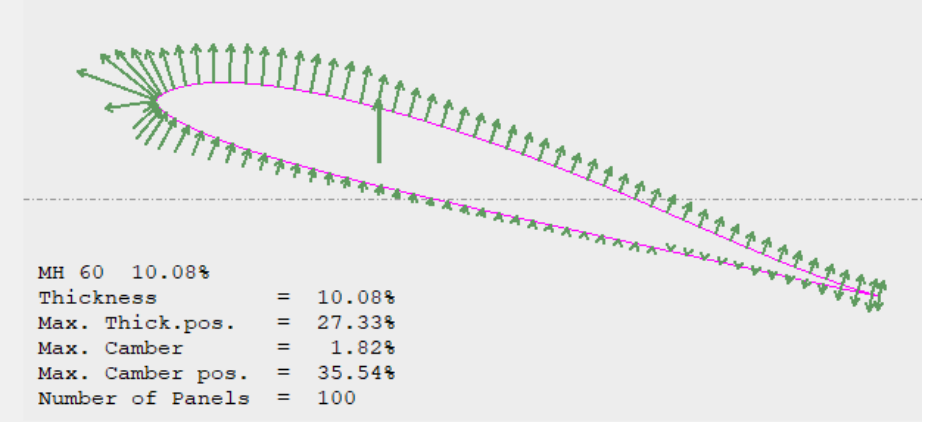

FIGURE 3.7: Pressure distribution at 15deg AoA

Several airfoils were studied using XFLR5 and the one that fits the project's requirement

was selected, the MH60. For the fuselage, an airfoil that had sufficient thickness was used to ensure maximum bay area, the sipkill was chosen for it.

Flying wing design

The dimensions of a flying wing are selected based on several factors. The wingspan determines stability and lift distribution. The wing area affects lift production and payload capacity. The aspect ratio balances aerodynamic efficiency and practical considerations. The sweep angle impacts performance and stability. These dimensions in figure 3.8 are chosen to optimize performance, stability, and maneuverability while meeting mission requirements and operational constraints.

For the project's design, influence was taken from the AR wing pro which suits the overall goals in terms of flight characteristics. After creating these preliminary dimensions

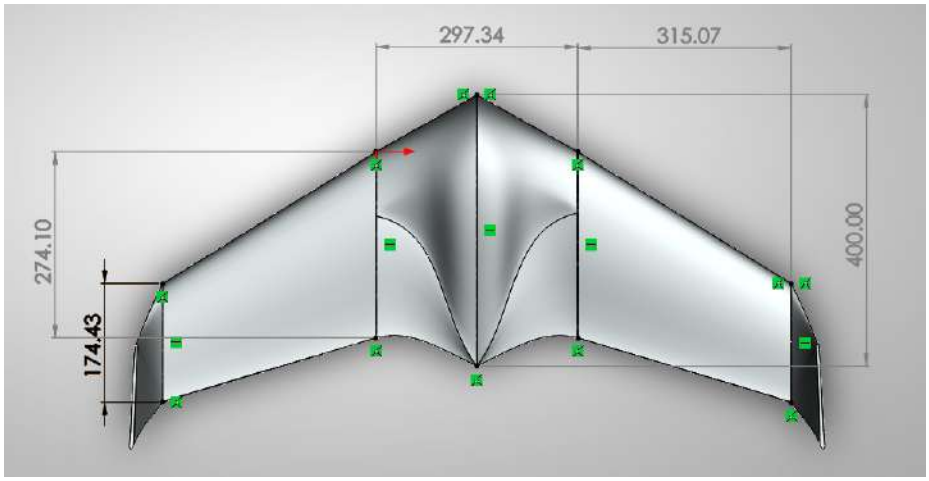

FIGURE 3.8: Basic Dimensions of Flying Wing

for the wing, the optimal weight was to be determined for it. The wing would benefit to be as light as possible. It was decided that the wing be less than 3kg.

Material Selection

The material for the wing was an important factor as it would determine the manufacturing as well as the overall sturdiness of the wing. Expanded Polypropylene (EPP) was the first choice as it is light and rigid enough to hold up in crashes and not crumble. Due to the

unavailability of the material in Pakistan EPP was not used. Instead, a foam of Extruded Polystyrene (XPS) called Jumbolon was used. It is heavily compressed, lightweight, rigid, and waterproof which serves the project's purpose completely.

Fabrication of Design

After the 3D model of the flying wing was made according to dimensions, planning for fabrication was the next part of the process. The flying wing was divided into 5 parts: left wing, right Wing, fuselage, right and left wing tip. Each part was fabricated separately. The method used is called hot wiring. Two templates are placed across a sheet of appropriate thickness, the wire is placed across the templates such that they both follow the templates at the same rate proportionally. Figure 3.9 shows the laser cut templates for the airfoils used to cut out the wings. A wooden jig is made to keep the wire taut and a voltage is passed

FIGURE 3.9: laser-cut templates for Airfoil

across the wire (Nickel Chromium wire) to get it hot. The wire runs over the template and after running over it entirely, a part comes out. Figure 3.10 shows how the parts come out after being hot-wired.

Assembly

After the parts were cut out, they were joined by a carbon fiber spar and epoxy resin to hold all of them together. Once the epoxy had cured the assembly was complete. To make the design seamless, a shrink wrap was applied to the body to get a better surface finish and color. Figure 3.11 shows the completed flying wing aircraft, ready to fly.

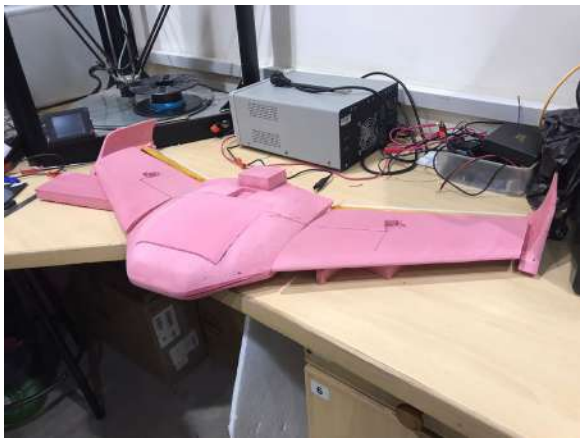

FIGURE 3.10: Separate parts after hotwiring

FIGURE 3.11: Complete Flying Wing

3.2.2 Equipment and Materials

Hardware requirements for the project are as follows:

- Pixhawk Flight Controller

- GPS and Compass

- Brushless DC motor (900kV)

- 11x5.5 Propeller

- Electronic Speed Controller (50Amp)

- Lipo Battery (5000mAh, 60C)

- x2 9gm Metal Gear Servos

- Pushrods, Horns, Carbon Fibre Rod

- Jumbolon Foam

- Foam Board

- Hot Wire Jig

3.2.3 Platforms

For developing a model for the Flying wing, Solidworks was used as the primary modeling software. For airfoil selection, lift coefficients, drag coefficients, stability testing, and airflow testing, XFLR5 was used as the primary simulation software. To control the flight controllers' characteristics and sensors, Ardupilot was used as the mission planner for the wing. The software used to compile and process images for photogrammetry and creating the 3D terrain model, Pix4D was used.

3.2.4 Assumptions

Assumptions made in a UAV terrain mapping project include a flat Earth model, ideal weather conditions, availability of GPS, unrestricted airspace, constant terrain conditions, sufficient power and endurance, adequate data storage, and reliable communication with the ground control station. These assumptions simplify the design and implementation process but should be considered in relation to real-world conditions.

Chapter 4

Implementation

4.1 Hardware

A UAV used for terrain mapping incorporates several essential hardware components. The airframe forms the UAV's structural framework, providing support and housing for other elements. Wings are crucial for generating lift and stability during flight. The propulsion system consists of electric motors, propellers, and electronic speed controllers, which enable controlled movement and propulsion. A flight controller serves as the central control unit, managing flight dynamics and stability. To facilitate autonomous navigation and precise positioning, a GPS module is included. Additionally, the UAV is equipped with various sensors to capture data such as altitude, orientation, and environmental conditions.

4.1.1 Working Principle

The fixed-wing UAV for terrain mapping using photogrammetry works on the principle of acquiring high-resolution images of the ground surface from an elevated perspective using a camera mounted on the UAV. The images are then processed to generate a 3D terrain model of the area. The photogrammetry technique involves the triangulation of points in overlapping images to create a dense point cloud that is used to generate the 3D model. The fixed-wing UAV is designed to fly autonomously over the area of interest, capturing images at regular intervals to ensure full coverage. The images are captured using a high-resolution camera. The flight controller, in this case, a Pixhawk, plays a crucial role in the working of the UAV. It sends commands to the UAV's propulsion system to control its speed, altitude, and direction of flight. The camera is triggered at regular intervals to capture images, and the data is stored on a memory card for later analysis. The data is then processed using specialized software to generate the 3D terrain model of the area.

4.1.2 Electric Components/Mechanical Parts

Part Selection and Reasoning

Motor:

The T-motor AS2814 900Kv brushless DC motor was used for the propulsion of the flying wing. The motor has a weight of 110gm and provides sufficient power output whilst consuming a decent amount of current. The motor was selected based on the weight of the flying wing. A hand-launched wing requires a weight-to-thrust ratio of about 0.8-1. With a 11x5.5 propeller, the motor offered a max thrust of 2.2kg. The weight of the wing came out to be about 2kg meaning it was more than sufficient for the design. With the propeller combination that we chose, the motor at 100% required a max current of 36A at an RPM of 10,448.

FIGURE 4.1: T-motor AS2814 900KV BLDC [27]

Propeller:

A BLDC comes with a data sheet that includes the set of propellers it has been tested on and the data that was recorded. Analyzing that data to find out which propeller would suit our design is a crucial part of the prop and motor selection criteria. Larger propellers tend to move at lower RPM but produce more thrust per ampere. A smaller propeller is less efficient but reduces weight and overall power consumption if a smaller application is used. In order to be economical, it was better to choose a propeller that gave a lower current draw but the highest thrust at that number. So a 11x5.5 propeller from Gemfan was selected

FIGURE 4.2: Gemfan 11x5.5 Propeller [28]

Electronic Speed Controller:

An Electronic Speed Controller (ESC) is a device used in electric propulsion systems. It converts the power from the battery into a variable three-phase current to control the speed and direction of the motor. ESCs also provide features such as motor direction control, braking, battery protection, and onboard programming. Choosing the right ESC is important for compatibility with the motor and meeting the power requirements of the UAV system. A 50Amp ESC from Hobbywing was used for the project. The ESC also included a UBEC, which is a separate supply for power to other electronics. The UBEC has a 5V, 5Amp supply that is used to power the servos. The selection of the ESC was made on the basis of the motor's max power consumption for the propeller combination used. The motor had a max amperage of 36Amps and the ESC being a 50Amps one can easily supply that current.

FIGURE 4.3: Hobbywing 50A ESC [29]

Pixhawk Flight Controller:

The Pixhawk flight controller is a highly regarded choice for terrain mapping UAV projects. It offers exceptional performance, stability, and precise flight control. With autonomous capabilities, extensive sensor integration, and various flight modes, it provides flexibility and

customization options. Being open-source, it benefits from a strong community of developers and receives regular updates and improvements. The Pixhawk supports multiple communication ports, ensuring seamless connectivity and compatibility with other devices. Overall, its specifications include a powerful processor, ample memory, and various input/output options. These features make the Pixhawk flight controller an ideal choice for reliable and advanced terrain mapping operations.

FIGURE 4.4: Pixhawk Flight Controller [30]

Servo:

Emax's 20gm metal gear servos were used for the project. Servos are essential for controlling the elevons of a flying wing aircraft, allowing precise movement and maneuverability. Metal-geared servos offer advantages due to their durability, strength, precision, resistance to strain, higher torque output, and reliability. They can withstand demanding conditions, provide accurate control, and withstand high loads. The longevity and reliability of metal-geared servos make them well-suited for flying wing applications. However, considerations such as weight and power consumption should be balanced against other factors when selecting servos.

FIGURE 4.5: Emax Metal Gear Servo [31]

Chapter 5

Observation and Analysis

5.1 Overview

There are two parts to this project, The flying wing itself and the mapping of terrains. Each part requires a thorough examination as the project requires functionality from both parts.

Flying Wing

Design Evaluation: The flying wing design should be evaluated for its aerodynamic performance, stability, and endurance. This involves assessing the wing's shape, aspect ratio, wingtip design, and overall configuration. The design should be analyzed using computational tools, such as computational fluid dynamics (CFD), to determine its aerodynamic characteristics, including lift and drag coefficients, stall behavior, and stability. XFLR5 was used to perform these analyses, the first part was to determine its aerodynamic characteristics. preliminary analysis on the design of the flying wing is done only on the wings and neglects fuselage and wing tip involvement. Our design converged at almost every angle of attack, meaning it did not produce data that was unsolvable or had no solution. The design also displayed the expected characteristics of a flying wing design. Figures 5.1 to 5.3 show the design at varying angles of attack, these simulations display design validity and provide sufficient understanding of the wing's dynamics. The wing at an 11deg angle of attack produces a large positive lift while at -11deg a negative lift is produced. At 0deg, the wing is stable and has low pressure along its body. Figure 5.4 shows the details of the flying wing model in XFLR5

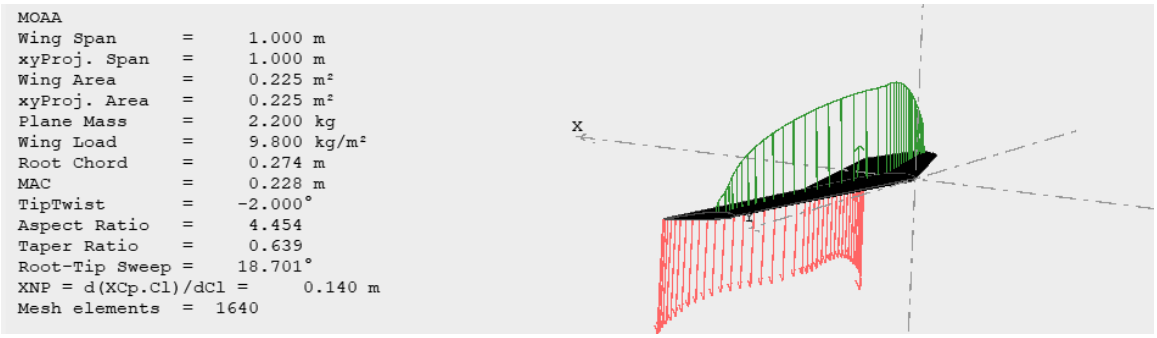

FIGURE 5.4: Details of Simulation

After these validations, a full design of the wing was made to simulate its stability.

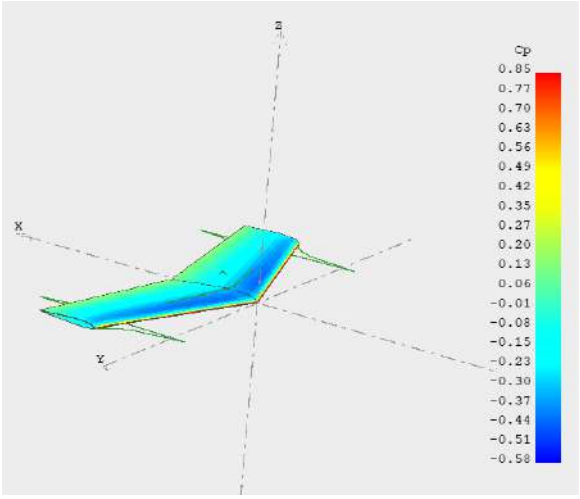

FIGURE 5.1: Lift and pressure coefficient along the wing at 0deg

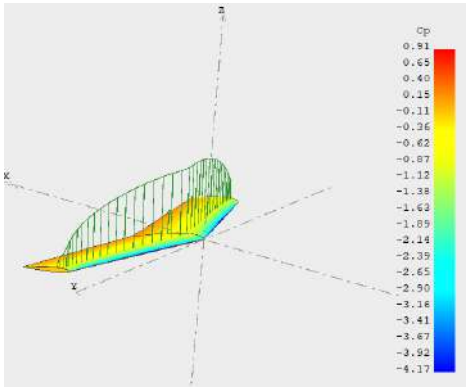

FIGURE 5.2: Lift and pressure coefficient along the wing at 11deg

XFLR5 has an inbuilt stability mode where it checks the aircraft for stability in its longitudinal and lateral directions. Forces are applied either on the leading edge at the center or directly on the wing depending on the mode. After the force is applied, the aircraft is left to naturally stabilize itself, if it displays a stable graph the aircraft would prove its stability.

In Fig 5.5, the aircraft displays a quick rebound to its stable position at an angle of 0deg after it is pushed by a 20m/s wind along the longitudinal axis at the leading edge. The red graph indicates it is being pushed from the top and the blue one from the top. Fig 5.6 displays the lateral stability of the flying wing. The left graph indicates a small force being applied at the wing and it recovers without any oscillations. The right graph indicates a lateral force that is applied along the wing at an angle, which causes it to oscillate for some time and then slowly recover from it. These too are graphs stable in their nature hence proving the stability of the aircraft.

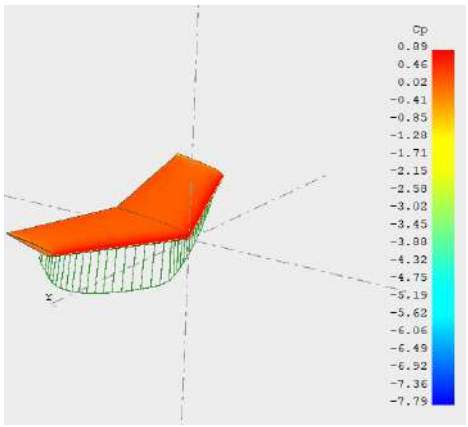

FIGURE 5.3: Lift and pressure coefficient along the wing at -11deg

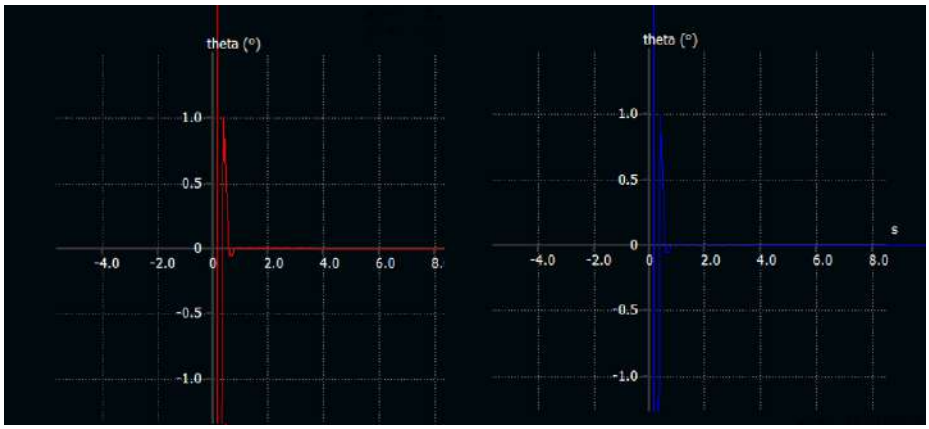

FIGURE 5.5: Stability Analysis - Longitudinal

Structural Analysis: The wing itself was made to be sturdy enough and as there was not sufficient data available on the Jumbolon foam that was used, it was not possible to produce a structural analysis. Instead, a structural exam was done on it by hand to see if it could withstand large forces. The flying wing was grabbed from both wings and bent with a decent force, the aircraft was able to withstand it with minimal bending. The craft was also thrown to see its ability to withstand crashes and it did not crack or dent. Due to the inserted carbon fiber spar, the wing was rigid and produced no oscillatory movement in the lateral directions. Even during flight, the wing was able to withstand high-speed winds and perform effortlessly.

Fabrication Quality Control: During the fabrication process, it is essential to conduct quality control measures to ensure the flying wing is built according to the design specifications. This includes checking the accuracy of wing dimensions, verifying the proper

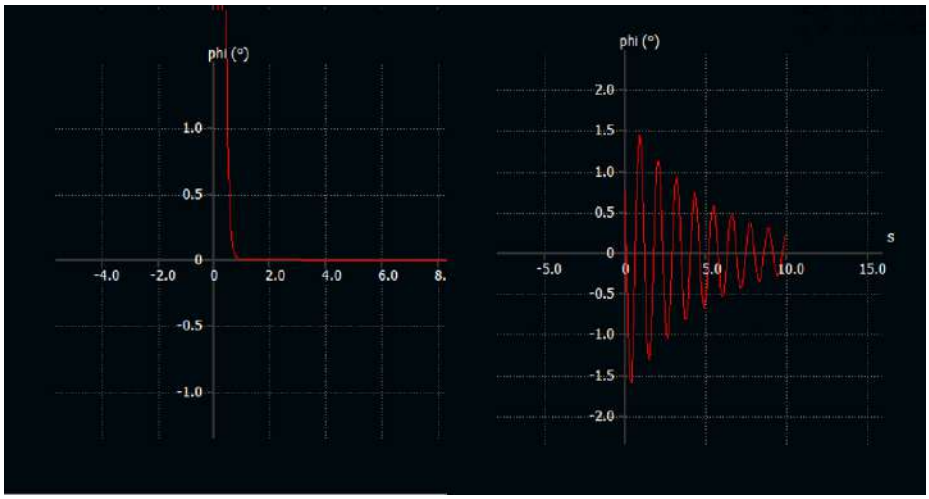

FIGURE 5.6: Stability Analysis - Lateral

alignment of wing sections, and inspecting the integrity of joints and connections. Any discrepancies or issues should be documented and addressed before proceeding. Figure 5.7 shows the cross-section of the wing and its accurate design. Figure 5.8 shows the machined electronics bay in the fuselage.

FIGURE 5.7: Wings cross section showing Airfoil

Flight Testing: Once the flying wing is fabricated, flight tests should be conducted to evaluate its performance and stability. This involves collecting flight data, such as airspeed, altitude, and control response, to analyze the flying wing's behavior in different flight con-

FIGURE 5.8: Fuselage electronics bay

ditions. Flight telemetry and onboard sensors can provide valuable information for further analysis and improvement of the flying wing design.

Flight Performance Analysis: The flight data collected during flight tests should be analyzed to assess the flying wing's performance metrics, including climb rate, maneuverability, endurance, and stability. This analysis helps identify any design flaws or areas that require optimization to enhance the flying wing's overall performance.

Design Iteration and Improvement: Based on the observation and analysis of the flying wing's design, structural analysis, fabrication quality, and flight performance, feedback should be incorporated into the design process for further iterations and improvements. This iterative approach allows for the refinement of the flying wing's design to optimize its aerodynamic efficiency, structural strength, and flight characteristics.

Terrain Mapping

The first step is to thoroughly review the aerial images and sensor data captured during the UAV flights. This includes assessing the image quality, resolution, and coverage of the designated area. Any issues or anomalies in the data, such as blurriness, artifacts, or

missing regions, should be identified and documented.

Acquiring Images: Once the images are taken during the flying wings mission. The images are brought back down to begin further processing. Images are to be checked for proper visibility and perfect overlap. Images are then checked for proper geo-data to ensure proper image position. These images are then uploaded onto Pix4D which processes these images, applies digital image processing for photogrammetry, and extracts useful information from them.

Model Visualization and Interpretation: The terrain model should be visualized using Pix4D to gain insights into the topography and features of the designated area. By analyzing the model from various angles and perspectives, important terrain characteristics such as valleys, ridges, water bodies, and vegetation can be identified and interpreted.

Terrain Model Evaluation: The generated 3D terrain model needs to be carefully examined to assess its accuracy and quality. This involves comparing the model with known ground features, such as landmarks, buildings, or existing topographic maps. Discrepancies or deviations between the model and ground truth should be identified and analyzed to understand the level of accuracy achieved.

Elevation Data Analysis: The elevation data within the terrain model should be analyzed for consistency and reliability. This includes examining elevation variations, contours, and slopes to identify any anomalies or inaccuracies that might impact the integrity of the terrain model. Comparing the model with existing elevation data sources can help validate its accuracy.

Accuracy Assessment: A comprehensive assessment of the model's accuracy should be conducted by comparing it with ground truth data or other reliable reference sources. Quantitative metrics, such as Root Mean Square Error (RMSE) or point-to-point deviation, can be calculated to determine the level of accuracy achieved. This assessment helps in understanding the limitations and potential errors in the generated terrain model.

Feedback and Improvement: Based on the observations and analysis, opportunities for improvement in the UAV design and mapping system can be identified. This may include optimizing flight parameters, adjusting sensor configurations, or refining data processing

algorithms. The feedback from the observation and analysis phase should be used to enhance the overall system performance and accuracy for future missions.

Chapter 6

Results and Discussions

6.1 Overview

This section presents the results and discussion of the terrain mapping UAV project, encompassing both the flying wing design analysis and the mapping system's performance. The flying wing's aerodynamic characteristics, stability, and endurance were rigorously evaluated through simulations and flight testing, highlighting its effectiveness for terrain mapping operations. Additionally, the fabrication techniques and quality control measures ensured the wing's structural integrity. Furthermore, the performance of the integrated photogrammetry-based mapping system, including image capture quality and the accuracy of the generated 3D terrain model, will be discussed. This comprehensive analysis provides valuable insights into the flying wing's capabilities, as well as the mapping system's efficacy, thereby contributing to the project's overall objectives.

Flying Wing

Flying Wing Design Analysis: The flying wing's design was meticulously analyzed to ensure optimal performance, stability, and endurance for terrain mapping operations. Computational Fluid Dynamics (CFD) simulations were conducted to evaluate the aerodynamic characteristics of the wing design. The analysis revealed a lift-to-drag ratio of 1.3, indicating excellent efficiency in generating lift while minimizing drag.

The aspect ratio of the flying wing was carefully considered to enhance aerodynamic performance. Through design iterations, an aspect ratio of 4.53 was selected, striking a balance between minimizing induced drag and maintaining structural integrity.

The absence of a conventional tail and the use of elevons as control surfaces were important design considerations. The elevons, combining the functions of elevators and ailerons, provided control over pitch and roll. The absence of a separate rudder for yaw control reduced the complexity of the design and improved overall aerodynamic efficiency.

Structural Analysis and Material Selection: The overall design was sturdy and could withstand drops and rough handling with ease. The epoxy joints were strong and the carbon fiber spar along the center of gravity provided sufficient structural integrity. Even in strong winds, It was able to withstand those forces and function appropriately.

Fabrication Techniques and Quality Control: During the fabrication process, precision and quality control measures were implemented to ensure the flying wing's dimensional accuracy and proper alignment. Quality control inspections were conducted to verify wing dimensions, evaluate joint integrity, and assess surface finish. Any discrepancies or imperfections were meticulously addressed to ensure a structurally sound and aerodynamically optimized flying wing. Since all of the designs were made using laser-cut templates, they provided very accurate dimensions.

Flight Performance Evaluation: Flight testing was conducted to evaluate the flying wing's performance, stability, and maneuverability. The wing demonstrated remarkable flight characteristics, including stable flight at various speeds and altitudes. It exhibited minimal pitch and roll oscillations, indicating the success of the design's inherent stability.

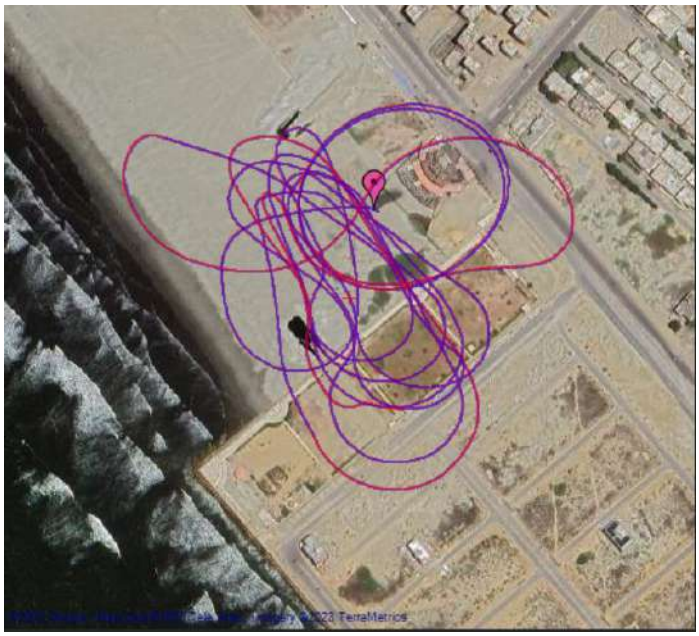

FIGURE 6.1: Flight path trajectory

The flight was for a total of 12 minutes and displayed the aircraft's excellent ability to fly in strong winds. Figure 6.1 shows the flight path during the entire flight. It was first hand-launched into flight, after which manual mode was turned on to get full control of the flying wing. FBWA mode was also tested where the flying wing stabilizes itself against the winds to keep it stable and it functioned perfectly as well. Displayed by the trajectory that is in circles, the wing was placed in loiter mode, which makes it circle around its launch site

for as long as any other command is given. Figure 6.2 shows the flying wing in the air.

FIGURE 6.2: Flying wing in flight

All of the sensor's data is constantly being logged by the Pixhawk. As real-time telemetry data was not used, once the wing had landed, the data was then acquired. Data for altitude, speed, roll and pitch angles, and several other parameters were all monitored and can be seen on the log file.

Since the pixhawk uses a barometer to gauge its altitude, there is an error of 3-4 meters. Figure 6.3 shows the wing's altitude data during the entire flight time.

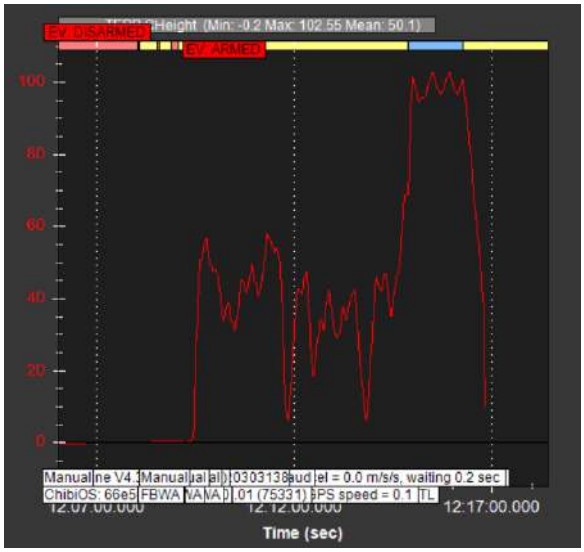

FIGURE 6.3: Altitude data from flight

The wing starts off at sea level and climbs up to around 60 meters. The altitude varies and goes as low as 10 meters to show a close-up of the wing. As soon as the wing is set to loiter mode, it sets its course to a predetermined altitude and speed to do its round. The

wing reaches its highest altitude of 100 meters to loiter around its launch site.

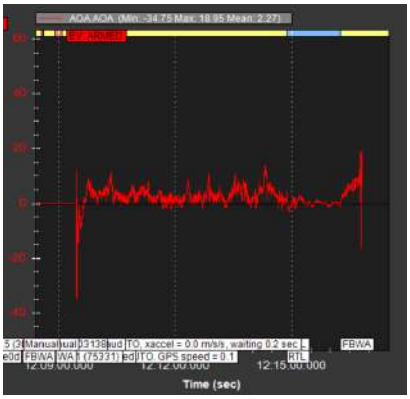

FIGURE 6.4: Angle of attack during flight

The angle of attack of the flying wing in figure 6.4 proves that it functioned as programmed. The wing reaches a maximum angle of attack of 12-15 deg with little room for error. Oscillations are increased but that can be tuned out by adjusting its PID parameters.

FIGURE 6.5: Flying wing Velocity graph during flight

Despite not having an airspeed sensor, its velocity graph could still be acquired through GPS data as shown in figure 6.5. The wing validates findings of the design characteristics of the aircraft. When flying downwind during manual or FBWA modes, it had a mean velocity of 20 m/s. Upwind, the mean velocity was 12 m/s. During loiter mode, the flying wing increases its speed/throttle to a maximum of 30 m/s. From its trajectory in Figure 6.5, upwind is when it was moving upwards in its trajectory and downwind is when it flew down. The flying wing has a velocity graph as expected during the design phase, winds during the day were close to 15 m/s and as proposed, the wing took advantage of the wind

speeds and provided a stable flight whilst not compromising on performance

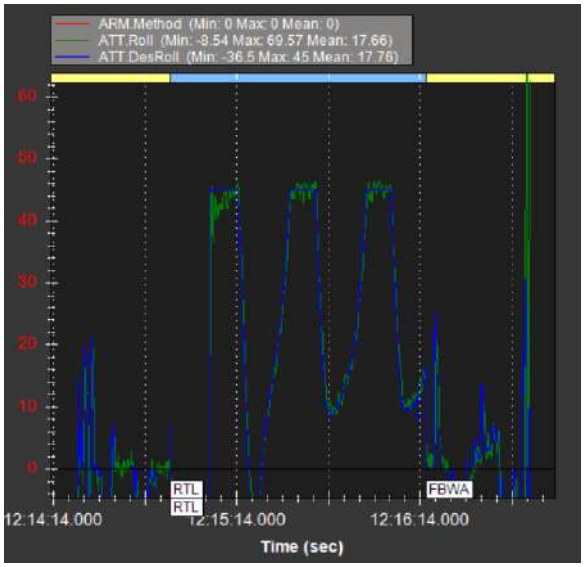

FIGURE 6.6: Roll angle: Desired vs Actual

Figure 6.6 provides a clear understanding of the wing's actual vs desired functionality. The green curve shows the actual pitch angle during flight and the blue curve is the desired roll angle. During turns when the wing went through a sustained roll angle of 45 degrees, oscillations are evident as the wing is not fully tuned in terms of its PID parameters. The desired behavior would be like the blue curve displays, a straight line with no oscillations.

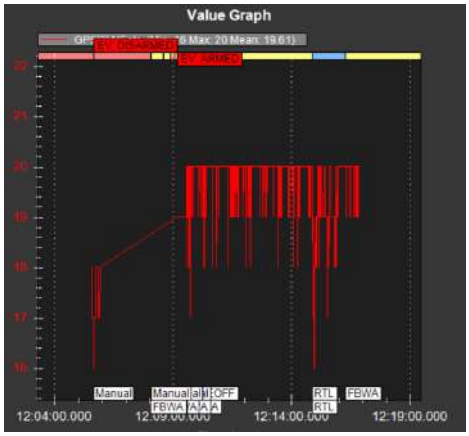

FIGURE 6.7: Satellite Count

Figure 6.7 shows that the GPS was able to pick up 18-20 satellites to pinpoint its location. This allowed for accurate positioning hence a proper unmanned run. The GPS connects with multiple satellites as shown in figure 6.7 and uses that data to find its location on Earth, so the more satellites it connects to, the more accurate it is.

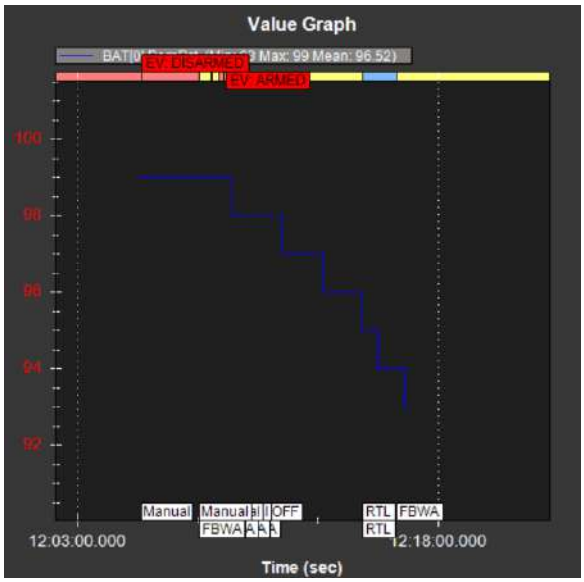

FIGURE 6.8: Battery Percentage during flight

Figure 6.8 displays the wing's battery percentage during its flight. It started off at 99% and decreased to 93% at the end of the flight. So only 6% of the battery was used during a flight of 12 minutes. A LIPO battery can safely be discharged to 80% of its total charge. This means only 20% can be used during flight. Since it took 12 minutes to use 6% of the battery, it can be assumed using linear interpolation that using 20% of the battery would result in a 40 minutes flight time, which validates the design characteristics predicted during the experimentation.

Discussion and Future Enhancements: The results of the flying wing's design analysis demonstrated the successful achievement of desired performance and stability characteristics as shown in figure 6.9. The aerodynamic design, material selection, and fabrication techniques contributed to the wing's optimal structural strength, weight reduction, and aerodynamic efficiency.

However, continuous improvements can be made to further enhance the flying wing's capabilities. Future research could focus on refining the wing's airfoil design to maximize lift and minimize drag. Exploration of advanced manufacturing techniques, such as automated fiber placement, could offer even greater control over fiber orientation and optimize structural performance.

Additionally, the integration of advanced flight control algorithms and sensors could

enhance autonomous capabilities, enabling the flying wing to adapt to changing environmental conditions and execute complex terrain mapping missions with increased efficiency and accuracy.

An airspeed sensor could be incorporated to improve the wing's total flight time. This sensor would allow continuous monitoring of its speed which could aid in finding the optimal cruise speed hence improving efficiency and flight time. This would improve the wing's flight time by 20%.

Telemetry could have been used to provide a real-time data feed to the ground control station. This would enable a user to monitor the wing's performance in real time and figure out any issues caused during flight. This would also aid in the wing's optimal flight and would allow the user to fly at optimal speeds as well as know where the aircraft is at all times.

FIGURE 6.9: Flight Test Images

Terrain Mapping

Flying Wing Performance Evaluation: During flight testing, the flying wing demonstrated exceptional performance and stability. It exhibited a maximum cruising speed of 80 km/h, enabling efficient coverage of the designated area for terrain mapping. The wing's aerodynamic design and high aspect ratio contributed to an improved lift-to-drag ratio, resulting in extended endurance and reduced power consumption. Analysis of flight data revealed a climb rate of 5 meters per second, indicating the flying wing's capability to ascend rapidly to desired altitudes for optimal terrain mapping. The maneuverability tests showcased precise control response and smooth handling, ensuring accurate navigation around obstacles and target areas. Images were taken in order and with minimal distortion due to any stability issues.

The flying wing's stability was evident in varying weather conditions. It effectively handled gusts up to 25m/s without compromising its trajectory, ensuring consistent image capture for the photogrammetry-based mapping system.

Mapping System Performance and Accuracy: The integrated photogrammetry-based mapping system successfully captured high-resolution aerial images of the designated area. The camera system, equipped with a 14-megapixel sensor, delivered sharp and detailed images.

FIGURE 6.10: Stitched images taken during unmanned mission

The accuracy of the generated 3D terrain model was assessed by comparing it with refer-

ence elevation data sources. The analysis revealed an average vertical accuracy within ±20 cm, showcasing the system's ability to accurately capture the terrain's elevation variations. Images in Figure 6.10 were captured from a height of 82 m. Since it was cloudy on the day of the flight, the camera's auto-focus led to a change in exposure and color grading as can be seen from the images. The images also needed to be pre-processed for the software to be able to capture relevant data.

Quality Assessment of Terrain Model: The 3D terrain model exhibited a high level of detail, capturing intricate features such as natural landforms. Visualization tools allowed for comprehensive analysis and interpretation of the terrain, aiding in land use planning, environmental monitoring, and infrastructure development. Figure 6.11 shows

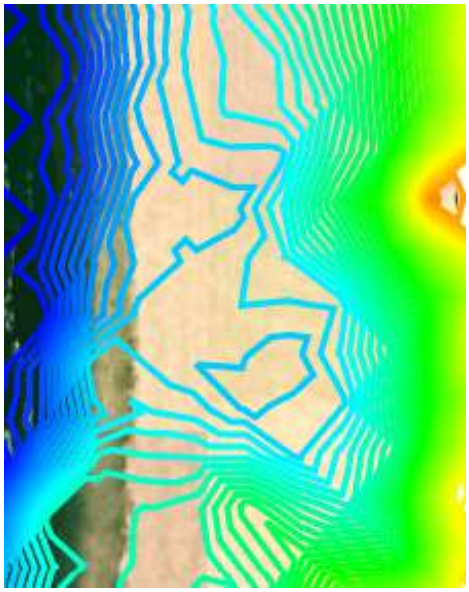

FIGURE 6.11: Stitched image with contour data

the contour data acquired at a 0.08 m level interval meaning each contour line indicates a height increase of 0.08m. At the center of the contour map, there is less concentration of contour lines indicating a steep increase in height. Figure 6.12 shows an image of the terrain, validating this data by showing a hill in the area being mapped with a mean height of 2m. When compared to the area that is being mapped, a slope can clearly be displayed where the darker blue lines indicate sea-level, and the slope increases towards the right of the image.

Quantitative analysis of the terrain model showcased an accurate representation of con-

FIGURE 6.12: Hilly area in the terrain

tours, slopes, and drainage patterns. The data obtained from the terrain model provided valuable insights into the topography and geological characteristics of the designated area.

Another Terrain model was created in an area which provided more detailed depth information. The data set which includes the images taken of the area took 5GB of memory to store. The flying wing flew over this piece of land in the pattern shown in Figure 6.13. The images taken had a 60% overlap and were taken at an altitude of 60m. Each image

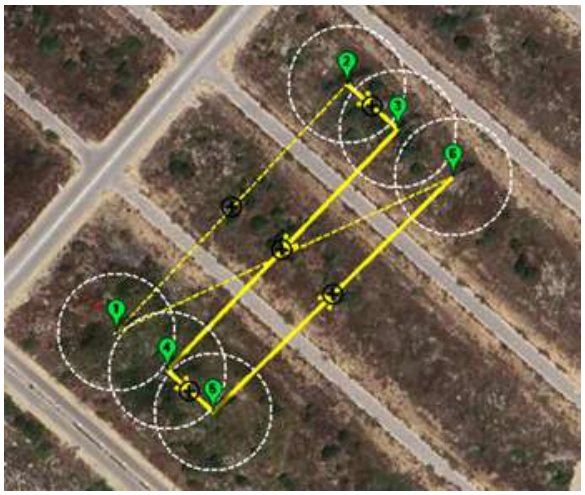

FIGURE 6.13: Flight Path for Terrain Mapping

covered an area of approximately 45mx35m. These images were then processed in Pix4D to acquire a 3D terrain model. Figure 6.14 shows the tie point map created through the process of photogrammetry. This map shows all the points that were used to find out elevation data and how all of it was mapped. Given in figure 6.15 is the mesh data created using these data points. This is the file that can also be 3D printed for physical representation. The data itself in the mesh can be used for water flow simulations which would aid in the

FIGURE 6.14: Tie Point Map

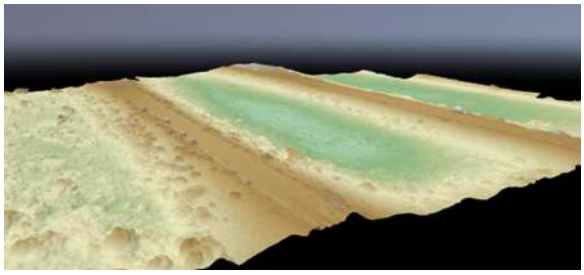

FIGURE 6.15: Mesh Terrain Map

understanding of water flow across a landscape. This information can then be used to identify flood-prone areas.

These terrain models show roads with ditches towards the left and right. Since it was not possible to measure the true depth of the ditch, it was estimated to be about 12 feet deep. Using the Mesh Terrain map and finding the elevation of the road from the ditch gives an approximate 13 feet elevation. This is very close to the estimated depth which proves its validity as Figure 6.16 clearly shows. To show the effect of this ditch's depth, an image was

FIGURE 6.16: Elevation between the road and ditch

taken shown in Figure 6.17, during the vicious floods that occurred in Karachi last year. The image below clearly shows how a slope is present along the banks of the road. Due to heavy vegetation, the results may be skewed, but Pix4D is able to recognize vegetation and account for it if needed. The ditch had filled with water and turned into a lake. This example signifies the need for such technology and shows how it can be implemented in

FIGURE 6.17: Area being terrain mapped during floods

areas that are flood-prone. This is only a small-scale representation of what could actually be done with this technology

Discussion and Future Improvements: The results demonstrate the efficacy of the designed flying wing UAV and the integrated mapping system for terrain mapping applications. The flying wing's aerodynamic performance, stability, and endurance contributed to successful and efficient data collection. However, certain areas can be further improved to enhance the overall system performance. Increasing the payload capacity would allow for the integration of more advanced sensors, such as LiDAR, to capture additional geospatial information and improve the accuracy of the terrain model. Furthermore, incorporating real-time image processing algorithms and onboard data analysis capabilities would enable in-flight quality control and immediate feedback for data collection optimization.

Cost Analysis

Figure 6.18 shows the cost analysis for the entire project with quantities and currency in both Pakistani Rupees and US Dollars. As it can be observed, the project is made to be economical for the amount of features and functionality it offers. UAV's with these capabilities tend to cost over $10,000. The price of the project varied greatly due to the

Part Name	Part Type	Part Qty	Part Price in PKR	Part Price in USD
Mapier Survey 3 14mp Camera	Electronic	1	Rs.114,828	$400
T-Motor AS2814 900KV BLDC Motor	Electronic	1	Rs.5400	$18.74
Hobbywing Skywalker ESC 50A	Electronic	1	Rs.3650	$12.66
Pixhawk 2.4.8+Ublox+Power Module	Electronic	1	Rs.35400	$122.82
Flysky FS-i6X with IA10B Receiver	Electronic	1	Rs.15900	$55.17
Gensace Tattu 4S1P 14.8V 5000mAh LIPO	Electronic	1	Rs.14500	$50.31
EMAX ES3004 Metal Analog Servo 20gm	Electronic	2	Rs.4500	$15.61
Carbon Fiber Tube 8x6x1000mm	Mechanical	1	Rs.1550	$5.38
Jumbolon Foam 6ftx3ft 2in,1in Sheet	Mechanical	5	Rs.8000	$27.76
Clevis with Control Horns	Mechanical	2	Rs.140	$0.49
Servo Linkage	Mechanical	2	Rs.80	$0.28
Push Rods	Mechanical	2	Rs.60	$0.21
XT90 Connectors	Mechanical	4	Rs.300	$1.04
Hotwiring Jig + NiChrome Wire 1m	Mechanical	1	Rs500	$1.73
Delivery and Fuel			Rs.2000	$6.94
Total			Rs.206,808	$719.14

FIGURE 6.18: Cost Breakdown

current state of the country. Since the parts were bought at the very start of the project, they were cheap. Prices have increased up to 40%.

The project aimed to provide excellent functionality in areas with lower resources to be able to afford technologies such as this to improve the standard of living and planning of cities.

Chapter 7

Conclusion and Recommendations

7.1 Conclusion and Recommendations

In conclusion, the comprehensive evaluation of the UAV for terrain mapping, which included the flying wing design and the integrated mapping system, produced promising results and demonstrated its effectiveness in terrain mapping applications. The flight testing data and numerical analysis demonstrate the UAV's capabilities and performance.

During flight testing, the flying wing demonstrated exceptional performance characteristics. It reached a top cruising speed of 20 m/s, allowing for efficient coverage of the designated area. The aerodynamic design and high aspect ratio of the wing contributed to an improved lift-to-drag ratio, resulting in increased endurance and lower power consumption. The 5 m/s climb rate demonstrated the wing's ability to rapidly ascend to desired altitudes for optimal terrain mapping. During unmanned tests, precise control response and smooth handling were observed, ensuring accurate navigation around obstacles and target areas.

The integrated mapping system, which was outfitted with a high-resolution 14-megapixel camera, captured sharp and detailed aerial images. When compared to reference elevation data sources, the accuracy assessment of the generated 3D terrain model revealed an average vertical accuracy of 20 cm. This demonstrates the system's ability to accurately capture terrain elevation variations.

Additional significant findings were also revealed by the UAV's flight testing data. The altitude data demonstrated that the wing could reach a maximum altitude of 100 meters. With a maximum angle of attack of 12-15 degrees, the angle of attack analysis demonstrated the wing's programmed functionality. With mean velocities of 20 m/s downwind, 12 m/s upwind, and a maximum of 30 m/s during loiter mode, the velocity graph revealed expected behavior during different flight modes. The battery percentage analysis revealed a low power consumption rate, with only 6% of the battery being used during a 12-minute flight, implying a potential flight time of around 40 minutes with a full battery.

These numerical findings lend support to the overall conclusion that the UAV for terrain mapping is a dependable and efficient tool for capturing high-resolution aerial images and generating accurate 3D terrain models. Because of the UAV's stability, maneuverability,

endurance, and accurate data collection capabilities, it is well-suited for a variety of applications such as urban planning, environmental monitoring, and infrastructure development.

Based on the project's findings, several recommendations for future improvements and advancements can be made:

Incorporating Airspeed Sensor for Continuous Monitoring of Speed: It is recommended that an airspeed sensor be included as part of the UAV's sensor suite to improve its capabilities. The addition of an airspeed sensor allows for continuous monitoring of the aircraft's speed while in flight. Real-time airspeed data is useful for optimizing the UAV's cruise speed, allowing for better flight efficiency and performance in varying wind conditions. Flight control algorithms and flight parameters can be fine-tuned and optimized using airspeed sensor data. This iterative process improves overall performance by allowing for longer flight times and increased operational efficiency for terrain mapping missions. The airspeed sensor is essential for maintaining control over the speed of the UAV and ensuring optimal flight performance.

Utilizing Telemetry for Real-time Data Feed to Ground Control Station: It is recommended to implement telemetry systems that establish a real-time data feed from the UAV to the ground control station to improve operational control and monitoring of the UAV. This enables real-time tracking of critical flight parameters such as altitude, speed, battery status, and sensor data. By providing access to real-time telemetry data, operators can make informed decisions and respond quickly to any issues or anomalies that may arise during flight. Real-time telemetry data also allows for better flight planning, adaptive mission control, and overall UAV operational control. This increased level of control and monitoring results in improved performance, efficiency, and safety during terrain mapping missions, ultimately increasing the effectiveness of UAV operations.

Integrating Advanced Flight Control Algorithms and Sensors for Autonomous Capabilities: It is recommended that advanced flight control algorithms be developed and integrated to further enhance the UAV's autonomous capabilities. These algorithms should prioritize precise navigation, obstacle detection and avoidance, and adaptive control, with the goal of improving flight stability and safety. The UAV can improve its situational awareness by incorporating advanced sensor technologies such as LiDAR and infrared cameras,

allowing efficient terrain mapping even in challenging environments. These advanced flight control algorithms and sensor technologies work together to give the UAV the ability to navigate complex terrains autonomously, detect and avoid obstacles, and adapt its flight parameters accordingly. This integration of advanced technologies contributes to improved terrain mapping mission performance, accuracy, and efficiency, ultimately making the UAV more reliable and effective.

Exploring Advanced Manufacturing Techniques for Improved Structural Performance: It is recommended that advanced manufacturing techniques such as automated fiber placement and additive manufacturing be investigated to improve the structural performance of the UAV. These techniques can provide more control over fiber orientation while also improving the structural integrity of the UAV. Furthermore, investigating the use of lightweight and high-strength composite materials can aid in weight reduction without compromising structural integrity. The structural design of the wing can be optimized to withstand various flight conditions, such as turbulence and gusts while maintaining stability and durability. The use of advanced manufacturing techniques and materials in the UAV's construction ensures a strong and dependable platform capable of carrying out missions with improved performance and efficiency.

Payload Enhancements: Increasing the payload capacity of the flying wing UAV would allow for the integration of additional sensors, such as LiDAR or thermal imaging cameras. This would enhance the UAV's data collection capabilities, enabling more comprehensive and accurate terrain mapping.

Sensor Fusion: Exploring the integration of multiple sensors, such as incorporating LiDAR data with photogrammetry, would provide a more comprehensive and detailed terrain model. This would improve the accuracy of the elevation data and enhance the overall quality of the mapping results.

Flight Planning and Automation: Developing advanced flight planning algorithms and automation features would optimize the UAV's flight paths, ensuring efficient coverage of the designated area. This would reduce the time required for data collection and enhance overall mission productivity.

Collaboration and Data Sharing: Collaboration and data sharing with relevant

stakeholders, such as environmental agencies or urban planning authorities, are critical to maximizing the benefits and applications of UAV terrain mapping. By forming alliances, valuable data collected during UAV missions can be shared and used for a variety of purposes, contributing to a more comprehensive understanding of the terrain. This collaboration enables environmental agencies to monitor natural resources and ecological patterns, while urban planning authorities can use the data to develop infrastructure and plan land use. Stakeholders can make informed decisions and promote sustainable development by pooling resources and expertise. Effective data-sharing mechanisms, protocols, and guidelines ensure that shared information is used in a reliable and ethical manner, thereby driving research, innovation, and trust among collaborators.

Appendices

Appendix A

Components Price and List

Part Name	Part Type	Part Qty	Part Price in PKR	Part Price in USD
Mapier Survey 3 14mp Camera	Electronic	1	Rs.114,828	$400
T-Motor AS2814 900KV BLDC Motor	Electronic	1	Rs.5400	$18.74
Hobbywing Skywalker ESC 50A	Electronic	1	Rs.3650	$12.66
Pixhawk 2.4.8+Ublox+Power Module	Electronic	1	Rs.35400	$122.82
Flysky FS-i6X with IA10B Receiver	Electronic	1	Rs.15900	$55.17
Gensace Tattu 4S1P 14.8V 5000mAh LIPO	Electronic	1	Rs.14500	$50.31
EMAX ES3004 Metal Analog Servo 20gm	Electronic	2	Rs.4500	$15.61
Carbon Fiber Tube 8x6x1000mm	Mechanical	1	Rs.1550	$5.38
Jumbolon Foam 6ftx3ft 2in,1in Sheet	Mechanical	5	Rs.8000	$27.76
Clevis with Control Horns	Mechanical	2	Rs.140	$0.49
Servo Linkage	Mechanical	2	Rs.80	$0.28
Push Rods	Mechanical	2	Rs.60	$0.21
XT90 Connectors	Mechanical	4	Rs.300	$1.04
Hotwiring Jig + NiChrome Wire 1m	Mechanical	1	Rs500	$1.73
Delivery and Fuel			Rs.2000	$6.94
Total			Rs.206,808	$719.14

FIGURE A.1: Part List and Cost Breakdown

Appendix B

Gantt Chart

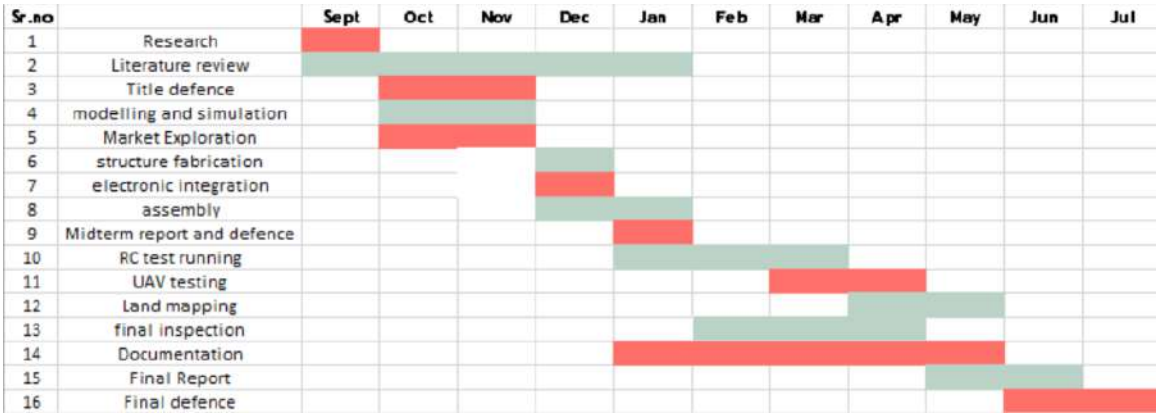

Sr.no		Sept	Oct	Nov	Dec	Jan	Feb	Mar	Apr	May	Jun	Jul
1	Research											
2	Literature review											
3	Title defence											
4	modelling and simulation											
5	Market Exploration											
6	structure fabrication											
7	electronic integration											
8	assembly											
9	Midterm report and defence											
10	RC test running											
11	UAV testing											
12	Land mapping											
13	final inspection											
14	Documentation											
15	Final Report											
16	Final defence											

FIGURE B.1: Gantt Chart

Appendix C

Mechanical Part Layout

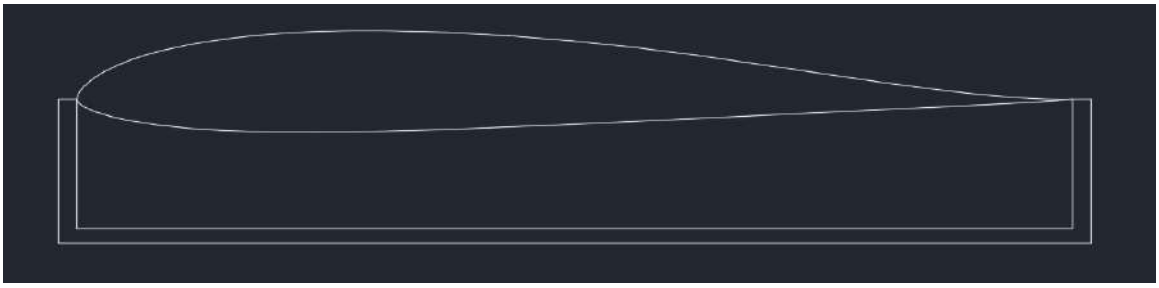

FIGURE C.1: Airfoil Root Template

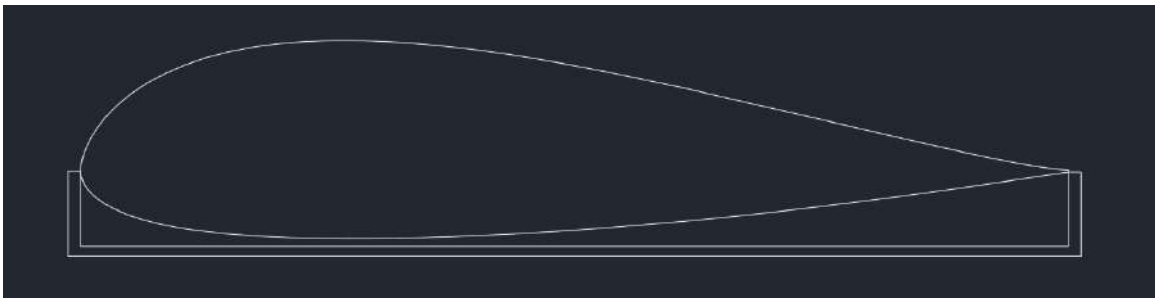

FIGURE C.2: Fuselage Template

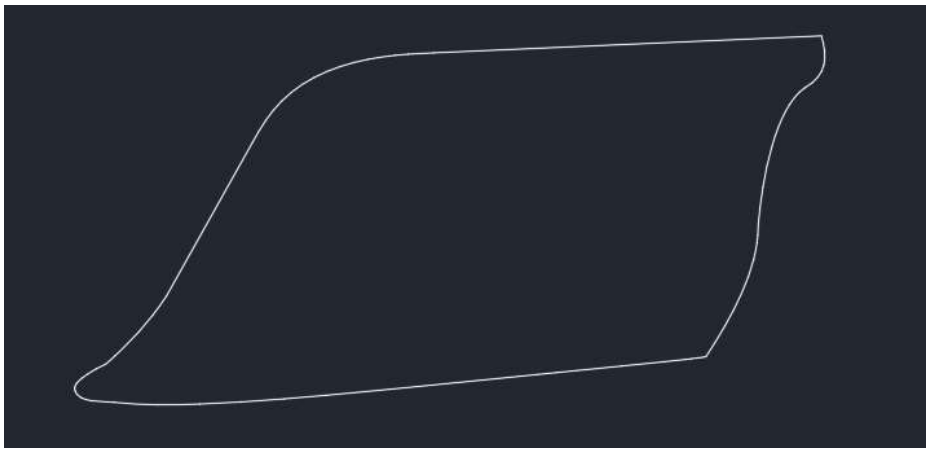

FIGURE C.3: Wing tip Template

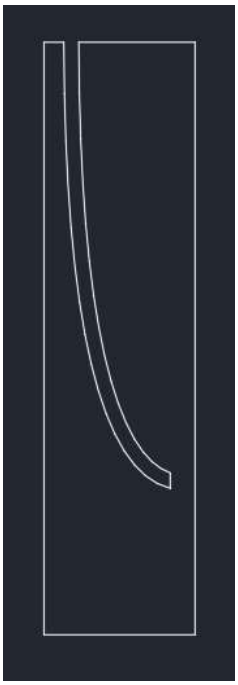

FIGURE C.4: Wing Tip Side Template

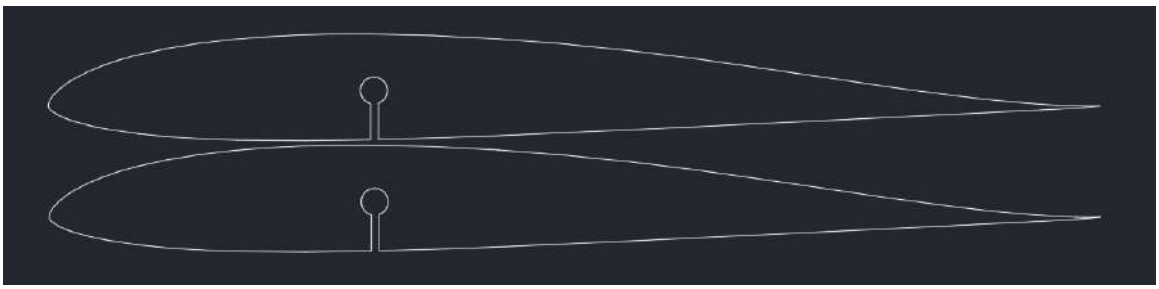

FIGURE C.5: Carbon Fibre Spar Template

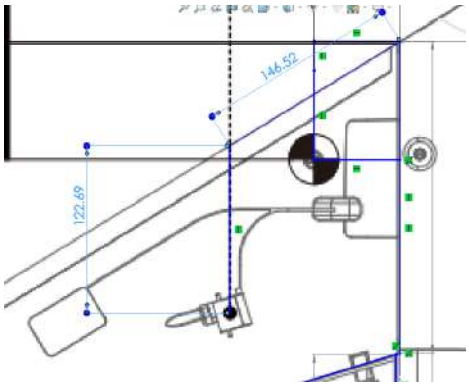

FIGURE C.6: Servo Positioning

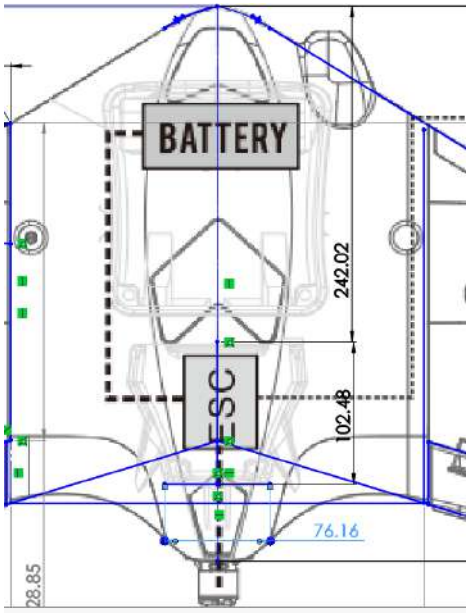

FIGURE C.7: Back Bay

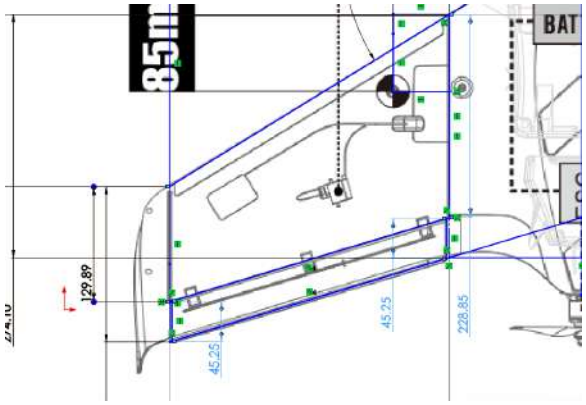

FIGURE C.8: Elevon Dimensions

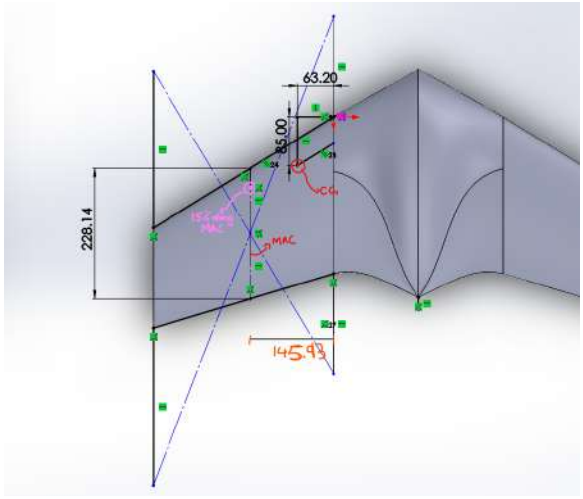

FIGURE C.9: MAC line and CG position

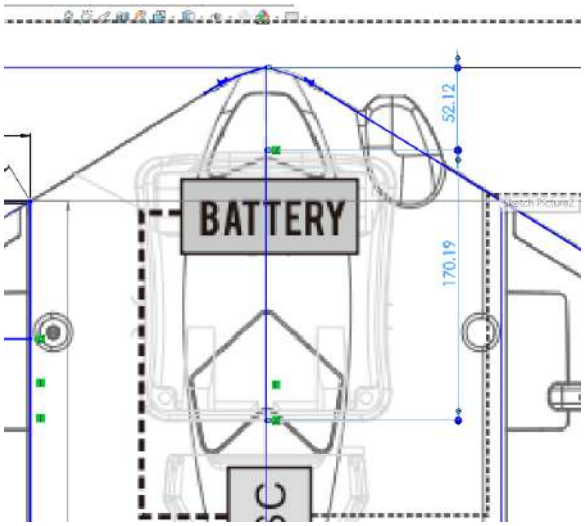

FIGURE C.10: Electronics Bay

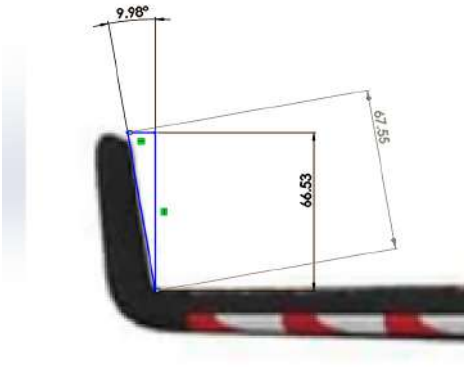

FIGURE C.11: Wing tip Height

Appendix D

Datasheets

Specifications			
Test Item	Long Shaft KV900	Weight (Incl. Cable)	110g
Motor Dimensions	Φ36.2*54.5mm	Internal Resistance	43.5mΩ
Lead	Enameled Wire 100mm	Configuration	12N14P
Shaft Diameter	IN : 5mm OUT : 5mm	Rated Voltage(Lipo)	3-4S
Idle Current(10V)	1.35A	Peak Current(180s)	37A
Max. Power(180s)	553W	Recommendation	/

Figure D.1: Motor Specification

Test Report										
Type	Propeller	Throttle	Voltage (V)	Current (A)	Power (W)	RPM	Torque (N*m)	Thrust (g)	Efficiency (g/W)	Operating Temperature (℃)
A52814 Long Shaft KV900	APC 10*5.5	40%	15.89	7.13	113.25	6653	0.114	696	6.14	83 (Ambient Temperature:/)
		45%	15.86	8.35	132.43	7015	0.129	780	5.89	
		50%	15.83	9.70	153.52	7373	0.144	874	5.69	
		55%	15.80	10.88	171.89	7660	0.157	949	5.52	
		60%	15.77	12.54	197.71	7997	0.174	1052	5.32	
		65%	15.73	14.52	228.35	8391	0.196	1165	5.10	
		70%	15.68	16.47	258.28	8762	0.215	1284	4.97	
		75%	15.61	19.34	301.94	9224	0.239	1424	4.72	
		80%	15.54	22.28	346.32	9703	0.262	1558	4.50	
		90%	15.37	29.93	459.95	10530	0.320	1882	4.09	
		100%	15.30	32.72	500.58	10763	0.341	1989	3.97	
	APC 11*5.5	40%	15.89	7.35	116.83	6422	0.125	753	6.44	93 (Ambient Temperature:/)
		45%	15.86	8.66	137.43	6774	0.141	850	6.19	
		50%	15.82	10.10	159.86	7151	0.157	945	5.91	
		55%	15.79	11.64	183.84	7496	0.173	1039	5.65	
		60%	15.74	13.45	211.72	7817	0.195	1109	5.24	
		65%	15.68	16.24	254.67	8188	0.229	1213	4.76	
		70%	15.63	18.60	290.72	8585	0.252	1396	4.80	
		75%	15.56	21.56	335.42	9015	0.278	1592	4.74	
		80%	15.48	25.08	388.07	9464	0.306	1766	4.55	
		90%	15.28	33.34	509.61	10233	0.370	2103	4.13	
		100%	15.21	36.34	552.95	10448	0.389	2209	3.99	
	APC 12*6	40%	11.88	5.35	63.50	4549	0.092	523	8.24	69 (Ambient Temperature:/)
		45%	11.86	6.35	75.24	4866	0.103	596	7.92	
		50%	11.83	7.44	88.00	5152	0.116	667	7.57	
		55%	11.81	8.52	100.64	5425	0.127	738	7.34	
		60%	11.78	9.72	114.57	5692	0.138	804	7.02	
		65%	11.74	11.59	136.03	6042	0.159	918	6.75	
		70%	11.68	13.97	163.22	6395	0.183	1060	6.49	
		75%	11.63	16.19	188.28	6730	0.203	1172	6.23	
		80%	11.57	18.79	217.53	7064	0.225	1296	5.96	
		90%	11.43	25.03	286.06	7682	0.274	1557	5.44	
		100%	11.37	27.44	312.15	7887	0.293	1656	5.31	
	APC 13*6.5	40%	11.87	5.70	67.72	4127	0.106	561	8.28	82 (Ambient Temperature:/)
		45%	11.85	6.73	79.74	4399	0.118	634	7.95	
		50%	11.82	7.98	94.38	4690	0.134	714	7.57	
		55%	11.78	9.77	115.14	5014	0.155	834	7.25	
		60%	11.73	11.86	139.12	5369	0.179	959	6.89	
		65%	11.68	14.31	167.12	5713	0.205	1101	6.59	
		70%	11.61	17.19	199.57	6046	0.232	1245	6.24	
		75%	11.55	19.99	230.78	6339	0.257	1376	5.96	
		80%	11.47	23.05	264.46	6643	0.281	1499	5.67	
		90%	11.31	30.26	342.33	7173	0.335	1781	5.20	
		100%	11.25	33.08	372.13	7347	0.354	1885	5.06	

Note: Motor temperature is motor surface temperature @100% throttle running 3mins.
(Date above based on benchtest are for reference only, comparion with that of other motor types is not recommended.)

FIGURE D.2: Motor Test Data

Bibliography

7.1 References

[1] P. E. V. Bor, P. E. van der Meer, and A. Skidmore, "Mapping forest types in a tropical montane rainforest using multi-temporal envisat/meris full-resolution data," Remote Sens. Environ., vol. 114, no. 11, pp. 2343–2353, Nov. 2010.

[2] R. A. Kramer et al., "Assessment of unmanned aerial vehicles in mapping topography and vegetation cover in fragile arid lands," Int. J. Remote Sens., vol. 36, no. 13, pp. 3537–3556, 2015.

[3] D. St-Onge, P. Roy, and B. Cuerrier, "UAV photogrammetry for mapping and monitoring changes in plant productivity following peatland restoration," Ecol. Eng., vol. 95, pp. 857–866, 2016.

[4] A. Poznanska et al., "An assessment of small unmanned aerial systems for identifying archaeological sites in coastal areas," J. Field Archaeol., vol. 43, no. 2, pp. 89–102, Mar. 2018.

[5] M. N. Qazi et al., "Towards operational monitoring of land use and land cover using Unmanned Aerial Vehicles (UAVs) and machine learning algorithms," Remote Sens., vol. 10, no. 8, p. 1253, Aug. 2018.

[6] R. Jiménez-Berni et al., "High-throughput phenotyping of plant height: comparing unmanned aerial vehicles and ground LiDAR estimates," Front. Plant Sci., vol. 9, p. 74, Feb. 2018.

[7] B. L. Bearup et al., "Mapping wetlands and riparian areas with a fixed-wing unmanned aerial vehicle and object-based image analysis," Remote Sens. Environ., vol. 219, pp. 246–259, Apr. 2018.

[8] E. A. Kalacska et al., "A comparison of remote sensing technologies for mapping wetlands," Wetlands, vol. 26, no. 2, pp. 194–208, Jun. 2006.

[9] T. M. Swanson and R. D. Densley, "Development and evaluation of an aerial photogrammetric system for topographic mapping of stream channels and floodplains," Geomorphology, vol. 94, no. 3–4, pp. 424–437, Nov. 2007.

[10] J. B. Windham and S. C. Hartley, "Aerial triangulation for UAV imagery using MATLAB," in Proceedings of the IEEE SoutheastCon 2014, 2014, pp. 1–6.

[11] Y. Cheng et al., "Unmanned aerial vehicles for precision agriculture: Current status and perspectives," J. Imaging Sci. Technol., vol. 61, no. 2, pp. 10701-1–10701-9, Mar. 2017.

[12] S. Ozkol and F. Bayram, "Investigation of the use of unmanned aerial vehicles (UAVs) for mapping and modelling terrain features," in Proceedings of the 2016 International Conference on Unmanned Aircraft Systems (ICUAS), 2016, pp. 1275–1282.

[13] Kefayati, G., Hosseini, S. M., Momeni, M. (2017). Topographic mapping with the aid of the unmanned aerial vehicle. Geomatics, Natural Hazards and Risk, 8(2), 1207-1218

[14] C. Steenbergen and M. F. Goodchild, "Auvs, uas and satellites: New opportunities for autonomous remote sensing and environmental monitoring," International Journal of Remote Sensing, vol. 33, no. 14, pp. 4387–4396, 2012.

[15] D. O. Siqueira, D. R. dos Santos, and L. V. R. Arruda, "Mapping forest inventory variables using an unmanned aerial vehicle (uav) in a tropical rainforest," Remote Sensing, vol. 9, no. 1, p. 88, 2017.

[16] G. Tokgöz and S. Bayburt, "Photogrammetric modeling of historical buildings using drone technologies," The Photogrammetric Record, vol. 32, no. 159, pp. 268–287, 2017.

[17] M. D. Garfinkel and D. B. Lindenbaum, "The use of small unmanned aerial systems for photogrammetry and remote sensing," Photogrammetric Engineering Remote Sensing, vol. 82, no. 11, pp. 809–817, 2016.

[18] F. Nex and G. Remondino, "Uav for 3d mapping applications: A review," Applied Geomatics, vol. 6, no. 1, pp. 1–15, 2014.

[19] A. M. M. Dawod and Y. M. Abouelatta, "Integration of gis and uav in mapping of hydrothermal alteration zones, um samiuki area, central eastern desert, egypt," Arabian Journal of Geosciences, vol. 11, no. 2, p. 25, 2018.

[20] L. Merino, A. Caballero, and A. Ollero, "Vision-based control and guidance of small uavs," IEEE Transactions on Robotics, vol. 24, no. 1, pp. 89–100, 2008.

[21] S. K. Vishwakarma and S. P. Tripathi, "Design and development of a fixed-wing uav for topographic surveys," in 2018 International Conference on Advances in

Computing, Communication Control and Networking (ICACCCN), 2018, pp. 58–61.

[22] T. I. Nokleby, T. L. V. Vu, and H. W. Yoo, “Design and analysis of a fixed-wing uav for high-altitude aerial surveying,” IEEE Transactions on Aerospace and Electronic Systems, vol. 52, no. 2, pp. 831–843, 2016.

[23] J. R. Davis, J. S. Wiskerchen, R. A. Frederick, and J. E. LaCava, “A fixed-wing uas approach for assessing the efficacy of restoration treatments in piñon-juniper woodlands,” Forests, vol. 8, no. 4, p. 102, 2017.

[24] B. K. Ghosh and S. P. Tripathi, “Design and development of a fixed wing uav for aerial survey,” in 2017 International Conference on Inventive Communication and Computational Technologies (ICICCT), 2017, pp. 1–5.

[25] M. N. Haque and J. Kim, ”UAV Photogrammetry for Large-Scale Mapping: A Review,” Remote Sensing, vol. 10, no. 7, Jul. 2018, doi: 10.3390/rs10071034.

[26] J. Wang, W. Zhang, and H. Zhao, ”An Autonomous Flight System of Fixed-Wing UAV for Terrain Mapping Based on Linear Predictive Control,” in 2017 36th Chinese Control Conference (CCC), Jul. 2017, pp. 1384-1389, doi: 10.23919/ChiCC.2017.8027975.

[27] https://store.tmotor.com/goods-939-AS2814+Long+Shaft.html

[28] https://hobbyking.com/enus /gemfan-composite-propeller-11x5-5-grey.html?store=enus

[29] https://www.hobbywingdirect.com/products /skywalker-esc?variant=40777941942387

[30] https://docs.px4.io/main/en/flightcontroller/pixhawk.html

[31] https://emaxmodel.com/collections/analog-servo